Insulin Potentiates JAK/STAT Signaling to Broadly Inhibit Flavivirus Replication in Insect Vectors

Laura R.H. Ahlers[1,6], **Chasity E. Trammell**[1], **Grace F. Carrell**[1], **Sophie Mackinnon**[1], **Brandi K. Torrevillas**[2], **Clement Y. Chow**[3], **Shirley Luckhart**[2,4], **Alan G. Goodman**[1,5,7,8,*]

[1]School of Molecular Biosciences, College of Veterinary Medicine, Washington State University, Pullman, WA 99164, USA

[2]Department of Entomology, Plant Pathology, and Nematology, College of Agricultural and Life Sciences, University of Idaho, Moscow, ID 83844, USA

[3]Department of Human Genetics, University of Utah School of Medicine, Salt Lake City, UT 84132, USA

[4]Department of Biological Sciences, College of Science, University of Idaho, Moscow, ID 83844, USA

[5]Paul G. Allen School for Global Animal Health, College of Veterinary Medicine, Washington State University, Pullman, WA 99164, USA

[6]Present address: Laboratory of Infectious Diseases, National Institute of Allergy and Infectious Diseases, NIH, Bethesda, MD 20814, USA

[7]Lead Contact

[8]Twitter: @GoodmanLabWSU

SUMMARY

The World Health Organization estimates that more than half of the world's population is at risk for vector-borne diseases, including arboviruses. Because many arboviruses are mosquito borne, investigation of the insect immune response will help identify targets to reduce the spread of arboviruses. Here, we use a genetic screening approach to identify an insulin-like receptor as a component of the immune response to arboviral infection. We determine that vertebrate insulin reduces West Nile virus (WNV) replication in *Drosophila melanogaster* as well as WNV, Zika, and dengue virus titers in mosquito cells. Mechanistically, we show that insulin signaling activates the

JAK/STAT, but not RNAi, pathway via ERK to control infection in *Drosophila* cells and *Culex* mosquitoes through an integrated immune response. Finally, we validate that insulin priming of adult female *Culex* mosquitoes through a blood meal reduces WNV infection, demonstrating an essential role for insulin signaling in insect antiviral responses to human pathogens.

In Brief

The world's population is at risk for infection with several flaviviruses. Ahlers et al. use a living library of insects to determine that an insulin-like receptor controls West Nile virus infection. Insulin signaling is antiviral via the JAK/STAT pathway in both fly and mosquito models and against a range of flaviviruses.

Graphical Abstract
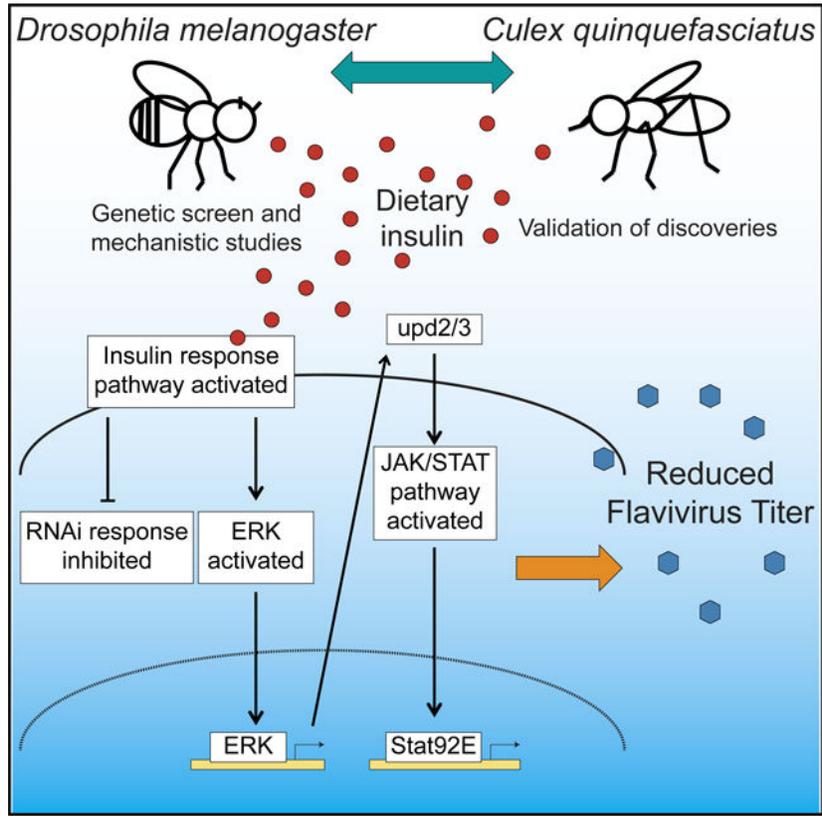
INTRODUCTION

The World Health Organization (WHO) estimates that more than half of the world's population is at risk for contracting a vector-borne disease. Mosquitoes are the most common insect vector, and they transmit the flaviviruses West Nile virus (WNV), dengue virus (DENV), and Zika virus (ZIKV). *Culex* spp. are important mosquito vectors and were the most frequently infected with WNV in the United States in 2017 (Centers for Disease Control and Prevention, 2018). Since 1999, WNV infection has caused disease in the 48 continental states, frequently resulting in mild febrile symptoms. In more extreme cases,

WNV causes neuroinvasive infection with severe complications and long-term patient consequences, including paralysis (Petersen et al., 2013). In 2017, the Centers for Disease Control and Prevention (CDC) reported 2,097 cases of human WNV infection in the United States, with 68% being classified as neuroinvasive (Centers for Disease Control and Prevention, 2018). DENV affects 390 million people worldwide each year (Bhatt et al., 2013). ZIKV, another arbovirus with significant health impacts, was originally confined to small outbreaks but expanded rapidly to more than 30 countries between 2015 and 2016 (Tham et al., 2018). Significantly, there are currently no post-exposure therapeutics or effective vaccines against WNV, DENV, or ZIKV, indicating an unmet need in public health.

Insects use broadly antiviral signaling pathways to respond to virus infection, most notably the RNAi response and the JAK/STAT pathways. *Drosophila melanogaster* activates RNAi as an innate immune response to DNA and RNA viruses (Bronkhorst et al., 2012; van Rij et al., 2006), specifically to WNV (Chotkowski et al., 2008), DENV (Mukherjee and Hanley, 2010), and ZIKV (Harsh et al., 2018). Subsequently it was shown that the RNAi pathway responds to WNV subtype Kunjin virus (WNV-Kun) infection in *Cx. quinquefasciatus* adult females (Paradkar et al., 2014). Studies using *D. melanogaster* found that RNAi pathway components communicate with non-canonical signaling proteins. For example, Deddouche et al. (2008) demonstrated that the gene *vago* is induced by *Drosophila* C virus (DCV) infection in a Dicer-2 (Dcr2)-dependent manner, and the transcription factor FoxO binds to the promoter regions of the RNAi components Dcr2, Argonaute 1 (AGO1), and AGO2 (Spellberg and Marr, 2015) during arboviral infection. Notably, WNV, DENV (Schnettler et al., 2012), and WNV-Kun (Moon et al., 2015) generate subgenomic flavivirus RNA (sfRNA) to antagonize the RNAi response and enhance virus survival. In addition, *D. melanogaster* uses the JAK/STAT pathway to respond to many RNA viruses, including DCV, cricket paralysis virus (CrPV), Sindbis virus (SINV) (Kemp et al., 2013), and ZIKV (Harsh et al., 2018), as well as the DNA virus invertebrate iridescent virus 6 (IIV-6) (West and Silverman, 2018). The JAK/STAT pathway is activated when secreted cytokines of the unpaired (upd) family engage the cell surface receptor domeless (dome) (Brown et al., 2001; Harrison et al., 1998). When activated, dome signals through the tyrosine kinase hopscotch (hop) (Binari and Perrimon, 1994) leading to phosphorylation of the transcription factor Stat92E (Yan et al., 1996). Stat92E controls the induction of genes that regulate cell proliferation, organismal growth, stem cell renewal, development, and immunity (Arbouzova and Zeidler, 2006). During viral infection in *D. melanogaster*, Stat92E induces *vir-1* (Dostert et al., 2005) and *Turandot M (TotM)* (Kemp et al., 2013), whose protein products have antiviral activity. *Aedes aegypti* uses the JAK/STAT pathway to respond to the flaviviruses WNV, DENV, and yellow fever virus (YFV) (Colpitts et al., 2011), and JAK/STAT signaling is responsive to WNV infection in *Cx. quinquefasciatus* cells (Paradkar et al., 2012). Although it is known that the RNAi and JAK/ STAT responses are important for controlling arboviral infection in insects, it is not fully understood how these pathways communicate with each other. Indeed, arboviruses are controlled by a number of different host responses, including 5′ to 3′ RNA decay (Molleston and Cherry, 2017), the *Vago*-mediated response, and the Dcr2-mediated response (Mussabekova et al., 2017). However, there may be additional, as yet unidentified, signaling components that contribute to the JAK/STAT or RNAi pathways for an integrated antiviral immune response.

Genetic variation in the human population contributes to disease progression for WNV (Bigham et al., 2011; Rios et al., 2010), DENV (Pabalan et al., 2017; Xavier-Carvalho et al., 2017), and ZIKV (Rossi et al., 2018). WNV causes symptoms in only 20% of infected individuals, (Hadler et al., 2014), with two-thirds of those cases becoming neuroinvasive (Centers for Disease Control and Prevention, 2018), DENV manifests in approximately 25% of individuals (Bhatt et al., 2013), and ZIKV is symptomatic in 18% of individuals (Duffy et al., 2009). Therefore, there is power in using genetic screens to uncover potential risk factors or gene mutations that contribute to flavivirus infection. For example, a genetic screen in humans revealed a SNP in *OAS1* that is associated with symptomatic WNV infection (Bigham et al., 2011). Rios et al. (2007, 2010) also identified mutations in equine *OAS1* that are associated with WNV disease. Similarly, genetic screens can be used to identify pathways that control innate immune responses or viral load in the arthropod vector (Kingsolver et al., 2013). Considering the remarkable genetic diversity of insect viruses (Li et al., 2015; Webster et al., 2015), the identification of antiviral pathways in insect vectors is important in understanding viral escape mechanisms or entry points and the development of viral control methods (Marques and Imler, 2016)

In this study, we used the *Drosophila* Genetic Reference Panel (DGRP), a fully sequenced, inbred panel of fly lines derived from a natural population (Mackay et al., 2012), to perform a pathway-unbiased screen for natural genetic variants associated with WNV-Kun infection. Through our screen, we found that the insulin-like receptor (*InR*) was necessary for host survival to WNV-Kun. Because mosquitoes are the natural vector for WNV-Kun and other flaviviruses, we leveraged fly genetics to investigate the insulin-mediated host response and address a relevant problem in global health. We determined that priming insect cells with vertebrate insulin activates insulin signaling through Akt and ERK and induces prolonged transcription of JAK/STAT-mediated antiviral genes. The effect of insulin priming was antiviral in both flies and mosquitoes and antiviral to other flaviviruses, namely ZIKV and DENV. This work identifies insulin signaling as a component of insect immunity to arboviral infection and demonstrates that insulin signaling works cooperatively with known antiviral immune pathways for host protection.

RESULTS

We used the DGRP (Mackay et al., 2012) and a corresponding genome-wide association study (GWAS) (Chow et al., 2013, 2016; Lavoy et al., 2018) to determine how natural genetic variation in flies can lead to inter-individual differences in survival during viral infection. The DGRP has been used to identify novel genes that respond to endoplasmic reticulum stress (Chow et al., 2013), bacterial infection (Bou Sleiman et al., 2015; Howick and Lazzaro, 2017; Wang et al., 2017), and lead toxicity (Zhou et al., 2016). Unbiased GWAS is informative in determining the genes associated with a particular phenotype and can identify novel genes connected with the phenotype of interest (Stranger et al., 2011). We performed our screen using the naturally attenuated WNV subtype Kunjin virus (WNV-Kun), which has high sequence identity to the lineage I WNV-New York 1999 strain (Lanciotti et al., 2002) and can infect *D. melanogaster* (Yasunaga et al., 2014).

We infected female flies from 94 of the DGRP lines with 10^4 plaque-forming units (PFUs) of WNV-Kun by intrathoracic injection (Yasunaga et al., 2014) and determined their mortality rates compared with flies treated with buffer only (mock infection) (Figure 1A). In this experiment, we used fly lines that were free of the endosymbiont *Wolbachia* because infection with this organism can protect against RNA virus infection (Teixeira et al., 2008). We monitored survival daily for 30 days and calculated the hazard ratio as a metric of survival (Figure 1B). We then used the log of the hazard ratio as the quantitative phenotype for the GWAS (Table S1), as described previously (Chow et al., 2013), and identified a set of genome-wide suggestive variants (nominal $p < 5 \times 10^{-5}$; Table S2), including *InR*. Next, we performed gene set enrichment analysis (GSEA) (Figure 1C) to identify groups of gene variants that were functionally enriched. Input for GSEA consisted of the gene and p value associated with each variant from the entire dataset. Given a defined set of genes annotated with a certain Gene Ontology (GO) function, GSEA determines how members of a GO category are distributed throughout the list of genes ranked by p value. GO categories enriched at the top of the list functionally describe the phenotype of the gene set (Subramanian et al., 2005). In the GO category regulation of cell proliferation (GO: 0008284), we identified genes that were previously shown to play a role in fly immunity to RNA virus infection via the JAK/STAT pathway (orange boxes), namely, *Stat92E*, *dome*, *upd3*, and *caudal* (*cad*) (Zhou and Agaisse, 2012). In addition to *InR*, we identified a number of insulin-like peptides (*ilps*) that were part of the functionally enriched GO categories female mating behavior (GO: 0060180) and hormone activity (GO: 0005179) (blue boxes). Functional enrichment of these *ilps* supported a role for insulin signaling in the antiviral immune response.

We selected *upd3*, *Stat92E*, *hop*, and *InR* for validation but also included *tak1* (TGFβ-activated kinase 1) and *egfr* (epidermal growth factor receptor) on the basis of previously identified roles for these genes in RNA virus infection (Xia et al., 2017). *Vir-1* is induced downstream of the JAK/STAT pathway (Kemp et al., 2013) and was used as a surrogate to validate this pathway. Fly lines with these genes deleted or knocked down by RNAi were infected with WNV-Kun. Because *upd2* and *upd3* have redundant roles (Kemp et al., 2013), we selected a line with mutations in both *upd2* and *upd3* for these analyses. Mortality rates for each genotype during WNV-Kun infection were compared with mock-infected (buffer only) controls. We used hazard ratio as a metric of survival because this value normalizes the mortality rates during virus infection to the mock-infected group and accounts for backgrounds that have different responses to mock infection. As expected on the basis of previous studies, JAK/STAT pathway mutants were susceptible to WNV-Kun infection on the basis of increased mortality ($p < 0.05$, hazard ratio > 1) in *upd ^{2}upd ^{3}* and *hop^3* mutants, while the control line y^1w^1 did not display significant mortality (Figures 2A–2C). Viral titers in *Stat92E^{HJ}* and *vir-1^{KG03668}* mutants were also increased at 5 days post-infection relative to controls, though not significantly (Figure 2D). Our data confirmed that knockdown of *InR* by RNAi (Figure S1) or *tak1^{2527}* mutation increased susceptibility to WNV-Kun infection (Figure 2E; Figure S2A), whereas the *egfr^{t1}* mutation, in contrast, did not display significant mortality (Figure S2B). Thus, we validated DGRP candidate genes *InR* and *tak1* as well as JAK/STAT pathway genes previously associated with RNA virus infection.

On the basis of validation of *InR* and the identification of *ilps* using GO analysis, we also determined that an *ilp7[1]* mutant is more susceptible to WNV-Kun infection compared with the control *w[1118]* background (Figure 2F). The *D. melanogaster* genome encodes for 8 ilps (Nässel and Vanden Broeck, 2016), and *ilp7* is the most conserved of the fly ilps and the only *ilp* that is truly orthologous to a mosquito *ilp* (Grönke et al., 2010). Because mosquitoes are exposed to exogenous insulin during a blood meal, and the aim of this work is to better understand the vector-host response during flavivirus infection, we subsequently tested the effects of insulin on the activation of Akt and WNV-Kun replication in *D. melanogaster* S2 cells and on virus replication in adult flies. The insulin signaling pathway in *D. melanogaster* is initiated by ilps binding to InR, which induces a phosphorylation cascade through the signaling protein chico, with subsequent bifurcation through two pathways, one of which is dependent on activation of PI3K (phosphoinositide 3-kinase), PDK1 (pyruvate dehydrogenase kinase 1), and Akt (Puig et al., 2003) and a second that is dependent on the activation of MAPK/ERK with feedback between the two branches (reviewed by Luckhart and Riehle, 2007). In addition to *D. melanogaster* ilps, the *D. melanogaster* InR has high affinity for bovine (Petruzzelli et al., 1985a, 1985b) and human insulin (Yamaguchi et al., 1995), and the binding of vertebrate insulin to the fly InR mediates the same signaling pathways (Yamaguchi et al., 1995). As in mosquitoes (Lim et al., 2005), the InR is expressed in the midgut and epidermis of *D. melanogaster* larva (Fernandez et al., 1995), and the midgut of adult flies (Choi et al., 2011). In *D. melanogaster* S2 cells, we observed robust Akt phosphorylation following 8 h of 1.7 μM insulin treatment (Figure 3A). Moreover, we observed reduced transcript levels of *InR* during exogenous insulin treatment, as measured by qRT-PCR (Figure S3). This was expected, as insulin-induced activation of Akt-mediated FoxO phosphorylation results in cytoplasmic retention of FoxO and a concomitant loss of FoxO-dependent *InR* induction (Puig et al., 2003). After 24 h of continuous insulin treatment prior to infection, WNV-Kun replication was also significantly reduced in S2 cells (Figure 3B), suggesting that insulin-mediated Akt activation stimulated an antiviral response. We tested insulin control of virus replication *in vivo* using WNV-Kun-infected OregonR flies raised on food containing 10 μM insulin. As in S2 cells, viral titer was significantly reduced in insulin-treated flies relative to control flies by 10 days post-infection (Figure 3C). This reduction in systemic replication of WNV-Kun can be attributed to the passage of ingested insulin from the midgut and dissemination to the hemolymph (Figure 3D).

We next investigated signaling crosstalk during insulin-mediated restriction of WNV-Kun replication, with particular focus on JAK/STAT, RNAi, and ERK signaling. We determined that insulin treatment induced prolonged transcription of JAK/STAT components *upd2*, *upd3*, and *TotM* (Figures 4A–4C), while significant *vir-1* induction was observed during insulin treatment only at 8 h post-infection (Figure 4D). In all cases, these effects were independent of virus infection (Figures 4A–4D). The RNAi components *AGO1*, *AGO2*, and *Dcr2* were induced at early times post-infection during insulin treatment (Figures 4E–4G). However, by 24 h post-infection, *AGO1* induction was significantly reduced during insulin treatment in both control and virus-infected cells (Figure 4E), *AGO2* induction was not observed in either cell treatment at 24 h post-infection (Figure 4F), and *Dcr2* induction persisted only in uninfected cells (Figure 4G). This is consistent with previous work

(Spellberg and Marr, 2015) in that all of these genes are regulated by the transcription factor FoxO but to different relative levels. Furthermore, in *D. melanogaster*, *Argonaute* levels are controlled by microRNA biogenesis, the ubiquitin-proteasome system, and even Dicer itself (Smibert et al., 2013). This study provides evidence of FoxO-independent regulation of RNAi genes, which may contribute to the varied transcription levels of *AGO1*, *Dcr2*, and *AGO2* in both our studies and those of Spellberg and Marr (2015). Together, our results suggested that insulin exposure prolongs the induction of JAK/STAT components, but not RNAi components, indicating that insulin sustains JAK/STAT signaling for the induction of antiviral immune genes.

To validate associations between insulin and JAK/STAT signaling, we examined temporal activation (phosphorylation) of ERK, Akt, and Stat92E in control and WNV-Kun-infected S2 cells with and without insulin treatment. ERK was phosphorylated during insulin treatment, as shown previously (Xu et al., 2013), and this phosphorylation was elevated during WNV-Kun infection relative to control (mock; Figure 4H, top row). Akt phosphorylation was induced by WNV-Kun infection, and this was enhanced by insulin treatment relative to control (Figure 4H, third row from top). Low levels of Akt activation were observed during infection in the absence of insulin, which was expected on the basis of previous results showing that WNV activates Akt (Shives et al., 2014). In support of a role for JAK/STAT signaling during insulin treatment, we immunoprecipitated Stat92E from whole S2 cell lysate to probe for tyrosine phosphorylation indicative of Stat92E activation. Similar to ERK, Stat92E was activated during WNV-Kun infection, and phosphorylation was enhanced relative to controls (mock) by insulin treatment (Figure 4H, bottom row).

Given that FoxO activity induces expression of RNAi components that are antiviral during CrPV infection (Spellberg and Marr, 2015), we sought to examine the role of FoxO during insulin treatment and WNV-Kun infection. For this purpose, a cohort of *D. melanogaster* engineered with a FoxO-GFP reporter was reared on food containing 10 μM insulin and infected as third-instar larvae with WNV-Kun. Given that the fat body is an important immune organ during viral infection in flies (Lautié -Harivel and Thomas-Orillard, 1990), we dissected this tissue to visualize FoxO-GFP localization by confocal microscopy from treated and control larvae. As expected on the basis of previous results (Puig et al., 2003), insulin treatment increased cytosolic FoxO-GFP, and this effect was independent of WNV-Kun infection (Figure 4I). Hence, insulin treatment results in a loss of FoxO-dependent transcription, consistent with the loss of induction of the RNAi components *AGO1*, *AGO2*, and *Dcr2* at 24 h post-infection during prolonged insulin treatment and infection (Figures 4E–4G).

We next asked if ERK phosphorylation leads to the transcription of JAK/STAT target genes for enhanced antiviral activity during insulin treatment. We determined that *D. melanogaster* S2 cells knocked down for ERK (Figure 4J) no longer express the genes encoding the JAK/STAT ligands *upd2* and *upd3* (Figures 4K and 4L) or the transcriptional target *vir-1* (Figure 4M) when treated with 1.7 μM insulin. Additionally, basal expression of *upd3* and *vir-1* is further reduced in cells knocked down for ERK compared with the scrambled double-stranded RNA (dsRNA) control (Figures 4L and 4M). Together, these results suggest that ERK activity can control JAK/STAT-mediated anti-viral pathways.

Because mosquitoes are the natural vectors for WNV, we sought to determine whether our findings in *D. melanogaster* would translate to mosquitoes. Akin to the fly model, the InR is expressed in the midgut of *An. stephensi* (Lim et al., 2005) and in the WNV vector *Cx. quinquefasciatus* (Nuss et al., 2018). Additionally, bovine insulin binds the *Aedes aegypti* InR (Brown et al., 2008), and human insulin persists in the *An. stephensi* midgut as intact peptide for up to 30 h after feeding and passes through the midgut into the mosquito body (including the head, thorax, and abdomen), where it can persist intact for at least 48 h after feeding (Drexler et al., 2013). Consistent with these observations, we determined that insulin treatment of *Cx. quinquefasciatus* Hsu cells, *Ae. aegypti* Aag2 cells, and *Ae. albopictus* C6/36 cells activated Akt (Figures 5A–5C) and reduced titers of WNV-Kun relative to control, untreated cells (Figures 5D–5F). This antiviral effect was not limited to WNV-Kun in that insulin treatment reduced the titers of two additional flaviviruses, ZIKV and DENV, in C6/36 cells (Figures 5G and 5H). Notably, C6/36 cells lack an RNAi response (Brackney et al., 2010), demonstrating that an RNAi response is not required for insulin-mediated antiviral activity. This is in contrast to Aag2 cells, which are RNAi competent (Scott et al., 2010) and display reduced WNV-Kun replication during insulin treatment, further suggesting that the effects of insulin are independent of RNAi-mediated antiviral activity. Finally, WNV-Kun titer was increased significantly in *Ae. albopictus* C6/36 cells treated with 10 μM MEK/ERK inhibitor U0126, and this treatment reversed the effects of insulin on virus replication (Figure S4), affirming that virus- and insulin-induced ERK activation (Figure 4H, top row) is functionally important in the regulation of virus replication in mosquito cells (Figure S4).

Last, we tested the effects of insulin treatment on WNV-Kun replication in *Cx. quinquefasciatus* adult females. Age-matched 6- to 9-day-old adult female mosquitoes were infected with WNV-Kun via blood meal in the presence or absence of insulin and collected at 1, 5, and 10 days post-infection (Figure 6A). Mosquitoes that did not blood feed were excluded from subsequent analyses. We selected 170 pM bovine insulin, as this dose is within the physiological range in humans (Darby et al., 2001) and activates insulin signaling and alters *Plasmodium falciparum* development in *Anopheles stephensi* (Pakpour et al., 2012). Similar to our results in *D. melanogaster*, we observed that insulin treatment led to decreased *R2D2* and *Dcr2* induction in insulin-fed control mosquitoes (Figures 6B and 6C), suggesting a reduced RNAi response in the context of increased *STAT* expression in insulin-fed infected mosquitoes (Figure 6D). Furthermore, WNV-Kun *env* and *NS5* gene expression levels were reduced in insulin-fed mosquitoes by 10 days post-infection (Figures 6E and 6F). Although insulin-induced *STAT* expression was significant at 1 day post-infection (Figure 6C), markers of virus infection were not significantly reduced until 10 days post-infection (Figures 6E and 6F). Intriguingly, numerous reports of WNV infection in mammalian cells indicate that WNV non-structural proteins, including NS5 for which expression increases over time in both control and insulin-treated mosquitoes (Figure 6F), can interfere with JAK/STAT signaling (Guo et al., 2005; Laurent-Rolle et al., 2010; Muñoz-Jordán et al., 2005), suggesting an explanation for the delay in observed effects of insulin on virus infection. Moreover, because of a point mutation in NS5, WNV-Kun displays reduced STAT antagonism (Laurent-Rolle et al., 2010), which allows a more robust JAK/STAT host response during infections with this strain compared with the virulent WNV strain NY99.

Collectively, these results suggest that vertebrate insulin ingested with the blood meal reduces viral RNA levels in the vector, perhaps through a STAT-mediated immune response that enables the vector to survive infection and transmit the virus to another host.

DISCUSSION

In the work presented here, we used the DGRP to investigate an antimicrobial host response to flaviviral infection and identified *InR*, along with other known antiviral response mediators, as components of the *D. melanogaster* response to WNV-Kun infection. We demonstrated that vertebrate insulin activates insulin and JAK/STAT signaling for a net antiviral effect in *D. melanogaster* cells. Moreover, an analogous antiviral effect is detectable in *Cx. quinquefasciatus*, *Ae. aegypti*, and *Ae. albopictus* cells, as well as *Cx. quinquefasciatus* females, and this insulin-dependent response is broadly antiviral to other flaviviruses, including DENV and ZIKV. Collectively, our data suggest that insulin activates known immune response pathways *in vitro* and *in vivo* for overall host restriction of flavivirus infection.

Mechanistically, we show that InR mediates its broad anti-flaviviral activity by selectively potentiating the JAK/STAT but not RNAi response. We show that ERK is activated in the context of FoxO inactivation and cytosolic localization, and we hypothesize that ERK links insulin signaling to the JAK/STAT pathway (Figure 7). Among elements related to JAK/STAT signaling in flies, upd2 controls ilp secretion by the fat body during the fed state (Rajan and Perrimon, 2012). The JAK/STAT-dependent genes *vir-1* and *TotM* are induced during RNA virus infection in *D. melanogaster*, with rapid-kill viruses (<10 days) inducing a *vir-1* response and slow-kill viruses inducing a *TotM* response (Kemp et al., 2013). WNV-Kun typically kills flies slowly, substantiating the prolonged *TotM* induction (Figure 4C) that we observed. This is in agreement with the findings of Harsh et al. (2018), in which a non-lethal ZIKV infection (strain MR755) induces a *TotM*, but not a *vir-1*, response. Given that MEKK1 signaling can contribute to *TotM* induction (Brun et al., 2006), ERK activation could prolong *TotM* induction during insulin priming to enhance an overall antiviral effect through JAK/STAT. In addition, we observed that ERK activation by insulin was induced concurrently with Stat92E phosphorylation (Figure 4H) and directly regulated virus replication (Figure S4), while FoxO activation and expression levels of RNAi components were reduced, suggesting that insulin activates the JAK/STAT pathway and ERK to control WNV-Kun replication. Interestingly, we observed that the antiviral RNAi response was not reliant on insulin signaling. This may be due in part to the fact that insulin signaling and a nutrient-rich environment lead to FoxO phosphorylation and reduced induction of FoxO target genes, such as *InR* and those that encode RNAi machinery (Puig et al., 2003; Spellberg and Marr, 2015). Although these conditions would lead to increased growth and lifespan regulation in *D. melanogaster* (Giannakou et al., 2004; Hwangbo et al., 2004) and mosquitoes (Arik et al., 2015; Kang et al., 2008), in the context of viral infection, they could be detrimental because of decreased antiviral RNAi activity. However, our results support a model in which insulin-induced JAK/STAT signaling compensates for the loss of RNAi activity. Importantly, we observed an insulin-mediated antiviral phenotype in both the RNAi-competent *Ae. aegypti* Aag2 cells (Scott et al., 2010) and RNAi-deficient *Ae. albopictus* C6/36 cells (Brackney et al., 2010), thus providing a natural experiment in support of our

inference that the insulin-dependent mosquito antiviral response is not mediated through RNAi.

We have determined that even hormonal levels of bovine insulin alter the host response enough to reduce WNV-Kun levels by a significant amount. Although this initially would seem disadvantageous to the pathogen in that there is apparently a lower capacity for virus transmission, the insulin-mediated host response may be protective enough to limit, but not eliminate, infection. If this were to occur, the infected vector could live long enough to feed again and transmit the virus to a new vertebrate host. This indicates a potential trade-off between immune response and pathogen/vector survival. In studies of potential trade-offs for the vector mosquito, WNV infection in *Cx. tarsalis* caused no change in survival but decreased fecundity and increased the feeding rate (Styer et al., 2007). In contrast, WNV-infected *Cx. pipiens* had no change in survival, fecundity, or feeding rate, but resistance to infection seemed to be associated with a fitness cost (Ciota et al., 2011). These studies suggest that the vector's response may affect the ability of the pathogen to infect a subsequent host. More work is needed to understand whether the insulin-mediated immune response in mosquitoes and reduction in flavivirus titer is beneficial to vertebrates, in that overall virus concentration is reduced in the insect and the capacity for transmission is lower, or if this effect is detrimental in that insulin reduces infection, resulting in mosquitoes that live longer and transmit the virus during subsequent blood feedings. These trade-offs could vary between mosquito species and between different flaviviruses.

Prior to our studies, the insulin signaling pathway had not been specifically linked to host immunity to WNV. Intriguingly, however, diabetes mellitus has been shown to increase risk for WNV infection (Nash et al., 2001), and in mouse models of the disease, leukocyte and T cell recruitment is decreased and WNV replication and neuroinvasiveness are increased in the absence of insulin (Kumar et al., 2012, 2014). These observations are mirrored in malaria parasite infection. Specifically, a higher percentage of *An. stephensi* becomes infected following feeding on *P. falciparum*-infected type 2 diabetic mice compared with mosquitoes that fed on control animals, suggesting that diabetic mice are more efficient at infecting mosquitoes (Pakpour et al., 2016). Indeed, insulin signaling has previously been implicated in immunity to parasites, bacteria, and viruses in both insects and mammals. In *D. melanogaster*, Musselman et al. (2017) determined that insulin signaling is networked to peptidoglycan receptor signaling for an antibacterial immune response. In *An. stephensi*, overexpression of activated Akt in the midgut blocked *P. falciparum* infection (Corby-Harris et al., 2010). In human cells, Akt signaling has been connected to the immune response to the flavivirus hepatitis C virus (HCV) (Aytug et al., 2003), and virus-induced disruption of insulin signaling was observed to increase HCV replication (Zhang et al., 2018). A variety of studies suggest that insulin signaling-dependent activation of ERK contributes to this antiviral effect. In particular, ERK is activated in response to DENV in human cells (Smith et al., 2014), by WNV in mouse cells (Scherbik and Brinton, 2010), and by vesicular stomatitis virus (VSV), SINV, and DCV in *D. melanogaster* cells and in adult flies (Xu et al., 2013). Furthermore, Xu et al. (2013) showed that insulin- and ERK-dependent signaling restricts DCV and SINV infection in *D. melanogaster* and *Ae. aegypti* cells. Intriguingly, recent results indicate that the endosymbiont *Wolbachia* affects insulin signaling in mosquitoes. That work showed that *Wolbachia* downregulates *Aedes InR* expression and

reduces DENV and ZIKV replication (Haqshenas et al., 2019). Here, we investigated the role of exogenous insulin in *Wolbachia*-free insects and insect cells during flavivirus infection. Future studies of the effects of exogenous insulin signaling on flavivirus super-infection in *Wolbachia*-infected insects could further clarify insulin coordination of antiviral responses. Collectively, these previous studies and ours affirm that insulin signaling regulates innate immune responses to a broad array of microbial pathogens. Specifically, we propose that insulin integrates ERK and JAK/STAT signaling pathways during the host response to flavivirus infection.

Taken together, our data demonstrate that the *Cx. quinquefasciatus* response to insulin mirrors the *D. melanogaster* response in that JAK/STAT is induced by WNV-Kun infection and is potentiated by insulin in the blood meal, perhaps through ERK signaling. Given this signaling framework and the conservation of this antiviral effect, we have leveraged fly genetics to efficiently identify and validate across species the downstream mechanisms that underlie insulin-dependent inhibition of viral replication. Although we are cognizant of species-specific distinctions that likely exist across an estimated 260 million years of evolution between flies and mosquitoes (Arensburger et al., 2010), we have provided an example of using these two systems in parallel to speed the identification of novel gene targets involved in the regulation of flavivirus infection in vector mosquitoes. Such findings could enhance novel genetic solutions to reduce mosquito-borne infections by targeting insulin signaling with small molecules (Zhang et al., 1999) or through the use of CRISPR in mosquitoes (Gantz et al., 2015). With respect to human infections, given that diabetes is a risk factor for flaviviral disease (Guo et al., 2017; Mavrouli et al., 2018) and that ERK- and Akt-dependent pathways control viral replication in human cells as noted above, *D. melanogaster* models of diabetes (Inoue et al., 2018; Musselman and Kühnlein, 2018) could extend our understanding of the mechanisms of increased risk for flavivirus infection and guide the identification of strategies to lessen human disease burden.

STAR★METHODS

LEAD CONTACT AND MATERIALS AVAILABILITY

Further information and requests for resources and reagents should be directed to and will be fulfilled by the Lead Contact, Alan Goodman (alan.goodman@wsu.edu). This study did not generate new unique reagents.

EXPERIMENTAL MODEL AND SUBJECT DETAILS

Fly Lines and Genetics—A genetic screen was completed using the available fly lines from the DGRP (Mackay et al., 2012) that lack the endosymbiont *Wolbachia* (Bloomington *Drosophila* Stock Center). RNAi knockdown of *InR* was achieved by crossing a driver line for actin (actin5C-GAL4) with a fly line containing a cassette expressing the UAS for actin and dsRNA for the *InR* gene. Progeny flies were knocked-down for *InR* if they contained the actin5C-GAL4 driver, and the sibling control flies contained wild-type levels of *InR* if they carried the *CyO* balancer. Knockdown of *InR* was confirmed by qRT-PCR (Figure S1). Flies used in the study are listed in the Key Resources table. Flies were maintained on standard cornmeal food (Genesee Scientific #66–112) at 25°C and 65% relative humidity, and a 12

h/12 h light/dark cycle. Adult flies used in experiments were all females, 2–7 days post-eclosion. Bovine insulin (Sigma 10516) was added to food preparation for a final concentration of 10 μM, within the range described in Xu et al. (2013). Dissemination of bovine insulin was determined by dissection of the midguts from five adult flies in PBS (Hiroyasu et al., 2018). PBS containing the hemolymph and carcasses were also collected, and all tissue was analyzed by western blot using an antibody against bovine insulin (Novus Biologicals NBP2–34260).

Bioinformatics—GWAS analysis was completed as described in Chow et al. (2013, 2016) and Lavoy et al., 2018), using log(hazard ratio) as a metric of mortality (Chow et al., 2013). All single nucleotide polymorphism (SNP) coordinates are based on the *D. melanogaster* dm6 genome build. Lines with less than 2% death in the mock-infected group were removed prior to analysis, as described (Chow et al., 2013). Gene Set Enrichment Analysis (GSEA) (Subramanian et al., 2005) was performed using all GWAS variant data and their associated p values as previously described (Subramanian et al., 2005). The gene nearest to each variant was assigned the variant's p value and used as GSEA input. While traditional GO analysis uses a set of genes based on a p value cutoff, GSEA examines the entire gene set (Dyer et al., 2008). A cut-off of $p < 0.01$ was used for the GO categories presented in Figure 1C.

Cells and Virus—Vero cells (ATCC, CRL-81) were kindly provided by A. Nicola and cultured at 37°C/5% CO_2 in DMEM (ThermoFisher 11965) supplemented with 10% FBS (Atlas BiologicalsFS-0500-A) and 1x antibiotic-antimycotic (ThermoFisher 15240062). *Aedes albopictus* C6/36 cells (ATCC, CRL-1660), which are free from persistent WNV, DENV, or ZIKV infection (Nag and Kramer, 2017; Nag et al., 2016), were cultured at 28°C/5% CO_2 in RPMI supplemented with 10% FBS (FisherScientific SH3007003HI), 0.15% sodium bicarbonate (ThermoFisher 25080), 1× non-essential amino acids (ThermoFisher 11140), 1× sodium pyruvate (ThermoFisher 11360), and 1× antibiotic-antimycotic. *Culex quinquefasciatus* Hsu cells (Hsu et al., 1970) were gifted by R. Tesh and cultured at 28°C in L-15 medium (ThermoFisher 11415) supplemented with 10% FBS (FisherScientific SH3007003HI), 10% tryptose phosphate buffer (ThermoFisher 18050), and 1× antibiotic-antimycotic. Hsu cells have been shown to be free of densoviruses, which are found in other mosquito cell lines (O'Neill et al., 1995). S2 cells were cultured as described in Ahlers et al. (2016) and are negative for Flock House virus infection. *Aedes aegypti* Aag2 cells (*Wolbachia*-free) were gifted by S. O'Neill and cultured as described in (Terradas et al., 2017). For insulin priming experiments, culture media with 2% FBS was supplemented with 1.7 μM insulin from bovine pancreas (Sigma 10516), as used previously (Zhang et al., 2011). Insulin was not cytotoxic to any of the insect cells used (Figure S5). For ERK inhibition experiments, culture media was supplemented with 10 μM U0126 in DMSO (Cell Signaling 9903) (Pakpour et al., 2012; Surachetpong et al., 2009) 24 hours prior to and during infection.

West Nile virus-Kunjin (strain MRM16) was provided by R. Tesh, passaged twice in Vero cells, and purified by ultracentrifugation. WNV-Kun can be used in arthropod containment level 2 (ACL2) facilities (Hackett and Cherry, 2018; U.S. Department of Health and Human Services, 2009). Zika virus (Paraiba strain) was gifted by S. Best, passaged once in C6/36

cells, and purified by ultracentrifugation. The Paraiba strain was isolated from a human patient during the Brazilian epidemic in 2015 (Tsetsarkin et al., 2016), and is virulent in mice (Marzi et al., 2018). Dengue virus 2 (New Guinea C strain) was gifted by S. Best. All experiments with a specific virus type utilized the same stock.

Mosquito Rearing—*Culex quinquefasciatus* eggs were originally collected near Johannesburg, South Africa and distributed by the Centers for Disease Control and Prevention by BEI Resources, NIAID, NIH (*Cx. quinquefasciatus*, Strain JHB, Eggs, NR-43025), and mosquitoes were reared following the conditions described by BEI and following Kauffman et al. (2017). Adult female mosquitoes were fed on defibrinated chicken blood (Colorado Serum Company 31141) in hog sausage casing. Adults were provided continuous access to sucrose (JT Baker 4072–01). 6–9 day old adult female mosquitoes were deprived of sucrose 48 hours prior to experimental feedings, as described (Moudy et al., 2009).

METHOD DETAILS

Plaque Assay—All data showing titers of KUNV, ZIKV, and DENV were determined by standard plaque assay on Vero cells (Baer and Kehn-Hall, 2014), with the exception of viral RNA levels in mosquitoes, which were determined by qRT-PCR.

Cytotoxicity of Bovine Insulin—Insulin or HEPES buffer control was added to a monolayer of cells in 48-well plates. Cells were collected at various times post-treatment, stained with trypan blue (ThermoFisher 15250–061), and scored as live or dead, as previously described (Ahlers et al., 2016). 8 technical replicates were averaged for each biological replicate.

Immunoprecipitation and Immunoblotting—Protein extracts were prepared by lysing cells with RIPA buffer (25 mM Tris-HCl (pH 7.6), 150 mM NaCl, 1 mM EDTA, 1% NP-40, 1% sodium deoxycholate, 0.1% SDS, 1mM Na_3VO_4, 1 mM NaF, 0.1 mM PMSF, 10 μM aprotinin, 5 μg/mL leupeptin, 1 μg/mL pepstatin A). Protein samples were diluted using 2× Laemmli loading buffer, mixed, and boiled for 5 minutes at 95°C. Samples were analyzed by SDS/PAGE using a 10% acrylamide gel, followed by transfer onto PVDF membranes (Millipore IPVH00010). Membranes were blocked with 5% BSA (ThermoFisher BP9706) in Tris-buffered saline (50 mM Tris-HCl pH 7.5, 150 mM NaCl) and 0.1% Tween-20 for 1 hour at room temperature.

Following insulin treatment and virus infection in *D. melanogaster* S2 cells, cells were lysed in RIPA buffer and 100 μg of total protein were immunoprecipitated with an antibody recognizing total Stat92E (Santa Cruz, sc-15708) at 4°C overnight, followed by a 2 hour incubation with Protein A agarose beads (Pierce 22811) at 4°C. Beads were washed three times with NETN buffer (20 mM Tris-HCl, pH 8.0, 100 mM NaCl, 1 mM EDTA, and 0.5% NP-40). Beads were boiled for 10 minutes at 95°C and supernatants were subjected to western blotting for P-Tyr (Cell Signaling 8954).

Primary antibody labeling was done with anti-P-Akt (Ser473) (1:2,000) (Cell Signaling 4060), anti-Akt (pan) (1:1,000) (Cell Signaling 4691), ERK (Cell Signaling 4695) (1:1,000),

P-ERK (Cell Signaling 4370) (1:2,000), P-Tyr (Cell Signaling 8954S) (1:2,000), or anti-actin (Sigma A2066) (1:10,000) overnight at 4°C. Secondary antibody labeling was done using anti-rabbit (Promega 4011) or anti-goat (Jackson Immunoresearch 705–035-147) IgG-HRP conjugate (1:10,000) by incubating membranes for 2 hours at room temperature. Blots were imaged onto film using luminol enhancer (ThermoFisher 1862124).

RNA Interference In Vitro—Long dsRNA targeting *D. melanogaster* ERK (*rolled*) and non-targeting control dsRNA was synthesized as described in Rogers and Rogers (2008). Primers are listed in the Key Resources table. dsRNA was transfected into S2 cells as described in Martin et al. (2018).

Quantitative Reverse Transcriptase PCR—qRT-PCR was used to measure gene mRNA levels in S2 cells and *Cx. quinquefasciatus*. Cells or mosquitoes were lysed with Trizol Reagent (ThermoFisher 15596). RNA was isolated by column purification (ZymoResearch R2050), DNA was removed (ThermoFisher 18068), and cDNA was prepared (BioRad 170–8891). Expression of *D. melanogaster* genes *InR*, *AGO1*, *AGO2*, *Dicer-2*, *upd2*, *upd3*, and *vir-1* were measured using SYBR Green reagents (ThermoFisher K0222) and normalized to *Rp49*. Expression of *TotM* was measured using primer/probe sets for *TotM* (Dm02362087_s1 ThermoFisher 4351372) and normalized to *RpL32* (Dm02151827_g1 (ThermoFisher 4331182), as in Kemp et al. (2013), using TaqMan Universal Master Mix (ThermoFisher 4304437). Expression of the *Cx. quinquefasciatus* genes *CxR2D2*, *CxDcr2*, and *CxSTAT* and of the WNV-Kun *envelope* and *NS5* genes was measured using SYBR Green and normalized to *Cx18S*. The reaction for both SYBR Green and TaqMan samples included one cycle of denaturation at 95°C for 10 minutes, followed by 40 cycles of denaturation at 95°C for 15 s and extension at 60°C for 1 minute, using an Applied Biosystems 7500 Fast Real Time PCR System. ROX was used as an internal control. qRT-PCR primer sequences are listed in the Key Resources table (Deddouche et al., 2008; Lin et al., 2004; Paradkar et al., 2012; Reid et al., 2015; Spellberg and Marr, 2015).

Larval Infections and Confocal Microscopy—Third-instar *D. melanogaster* larvae were washed with PBS, placed in a pool of buffer with WNV-Kun, and pricked with a tungsten needle (Hiroyasu et al., 2018). Fat bodies were dissected at 4 hours post-infection, fixed, and blocked following Loza-Coll et al. (2014). Samples were stained with DAPI, mounted onto coverslips using ProLong Diamond Antifade Mountant (Invitrogen P36961), and imaged using a Leica Sp8X confocal microscope.

Fly Infections—2–7 day old adult *D. melanogaster* were anesthetized with CO_2 and injected intrathoracically with 23 nL of WNV-Kun to achieve a dose of 10,000 PFU/fly, as described (Martin et al., 2018; Yasunaga et al., 2014). Mock infection was the equivalent of injection with saline. For mortality studies, groups of at least 40 flies were injected and kept in vials containing cornmeal food (Genesee Scientific #66–112). DGRP survival curves were repeated to verify reproducibility. All survival studies for a specific mutant (e.g., *InR* RNAi or deletion mutants) were repeated and the survival data were combined. Vials were changed every three days. For viral titer experiments, three groups of five flies were collected, homogenized in PBS, and used as individual samples for plaque assay.

Mosquito Infections—WNV-Kun was added to chicken blood washed with RPMI, supplemented with 20% FBS and HEPES buffer or 170 pM insulin (Kang et al., 2008; Pakpour et al., 2012), at a final concentration of 1×10^7 PFU WNV-Kun/mL. The dose was selected as an intermediate between the doses used in Kilpatrick et al. (2008) and Paradkar et al. (2012). Female *Cx. quinquefasciatus* were maintained for three generations and subsequently fed using an artificial mosquito feeder (Chemglass Life Sciences) for 2 hours. Engorged females were separated under CO_2, placed in 1 gal cartons with continuous access to 10% sucrose, and collected at 1, 5, and 10 days post-infection for analysis. Females that did not feed were excluded from all subsequent analysis.

QUANTIFICATION AND STATISTICAL ANALYSIS

Results presented as dot plots show data from individual biological units (N = 3–9 replicates) and the arithmetic mean of the data, shown as a black horizontal line. Biological units of adult flies (N = 3–11 replicates) consisted of three to five pooled animals and biological units of mosquitoes (N = 3–6 replicates) consisted of three pooled animals. Results shown are representative of at least duplicate independent experiments, as indicated in the figure legends. All statistical analyses are performed on the biological unit/replicate scale and were completed using GraphPad Prism. Two-tailed unpaired t tests assuming unequal variance were utilized to compare normally distributed pairwise quantitative data. Two-way ANOVA with Tukey's correction for multiple comparisons was used to compare multivariate data. Mann-Whitney tests were utilized to compare distribution-free quantitative data. All error bars represent standard deviation of the mean. Any statistical outliers for experiments were identified using a Grubb's test ($\alpha = 0.05$) and removed. Survival curves were analyzed by the log-rank (Mantel-Cox) test using GraphPad Prism to determine p values between infected genotypes. When data from independently performed survival experiments are combined for a final curve, the maximum p value among the independent experiments is reported.

DATA AND CODE AVAILABILITY

All input phenotypic data (hazard ratios) are provided in Table S1. The full output GWAS data generated during this study are available at Mendeley Data (https://data.mendeley.com/datasets/xwzp5ymp24/3). This study did not generate code.

Supplementary Material

Refer to Web version on PubMed Central for supplementary material.

ACKNOWLEDGMENTS

REFERENCES

Ahlers LRH, Bastos RG, Hiroyasu A, and Goodman AG (2016). Invertebrate iridescent virus 6, a DNA virus, stimulates a mammalian innate immune response through RIG-I-like receptors. PLoS ONE 11, e0166088. [PubMed: 27824940]

Arbouzova NI, and Zeidler MP (2006). JAK/STAT signalling in Drosophila: insights into conserved regulatory and cellular functions. Development 133, 2605–2616. [PubMed: 16794031]

Arensburger P, Megy K, Waterhouse RM, Abrudan J, Amedeo P, Antelo B, Bartholomay L, Bidwell S, Caler E, Camara F, et al. (2010). Sequencing of Culex quinquefasciatus establishes a platform for mosquito comparative genomics. Science 330, 86–88. [PubMed: 20929810]

Arik AJ, Hun LV, Quicke K, Piatt M, Ziegler R, Scaraffia PY, Badgandi H, and Riehle MA (2015). Increased Akt signaling in the mosquito fat body increases adult survivorship. FASEB J. 29, 1404–1413. [PubMed: 25550465]

Aytug S, Reich D, Sapiro LE, Bernstein D, and Begum N (2003). Impaired IRS-1/PI3-kinase signaling in patients with HCV: a mechanism for increased prevalence of type 2 diabetes. Hepatology 38, 1384–1392. [PubMed: 14647049]

Baer A, and Kehn-Hall K (2014). Viral concentration determination through plaque assays: using traditional and novel overlay systems. J. Vis. Exp (93), e52065. [PubMed: 25407402]

Bhatt S, Gething PW, Brady OJ, Messina JP, Farlow AW, Moyes CL, Drake JM, Brownstein JS, Hoen AG, Sankoh O, et al. (2013). The global distribution and burden of dengue. Nature 496, 504–507. [PubMed: 23563266]

Bigham AW, Buckingham KJ, Husain S, Emond MJ, Bofferding KM, Gildersleeve H, Rutherford A, Astakhova NM, Perelygin AA, Busch MP, et al. (2011). Host genetic risk factors for West Nile virus infection and disease progression. PLoS ONE 6, e24745. [PubMed: 21935451]

Binari R, and Perrimon N (1994). Stripe-specific regulation of pair-rule genes by hopscotch, a putative Jak family tyrosine kinase in Drosophila. Genes Dev. 8, 300–312. [PubMed: 8314084]

Bou Sleiman MS, Osman D, Massouras A, Hoffmann AA, Lemaitre B, and Deplancke B (2015). Genetic, molecular and physiological basis of variation in Drosophila gut immunocompetence. Nat. Commun 6, 7829. [PubMed: 26213329]

Brackney DE, Scott JC, Sagawa F, Woodward JE, Miller NA, Schilkey FD, Mudge J, Wilusz J, Olson KE, Blair CD, and Ebel GD (2010). C6/36 Aedes albopictus cells have a dysfunctional antiviral RNA interference response. PLoS Negl. Trop. Dis 4, e856. [PubMed: 21049065]

Bronkhorst AW, van Cleef KWR, Vodovar N, Ince IA, Blanc H, Vlak JM, Saleh M-C, and van Rij RP (2012). The DNA virus invertebrate iridescent virus 6 is a target of the Drosophila RNAi machinery. Proc. Natl. Acad. Sci. U S A 109, E3604–E3613. [PubMed: 23151511]

Brown S, Hu N, and Hombría JC-G (2001). Identification of the first invertebrate interleukin JAK/STAT receptor, the Drosophila gene domeless. Curr. Biol 11, 1700–1705. [PubMed: 11696329]

Brown MR, Clark KD, Gulia M, Zhao Z, Garczynski SF, Crim JW, Suderman RJ, and Strand MR (2008). An insulin-like peptide regulates egg maturation and metabolism in the mosquito Aedes aegypti. Proc. Natl. Acad. Sci. U S A 105, 5716–5721. [PubMed: 18391205]

Brun S, Vidal S, Spellman P, Takahashi K, Tricoire H, and Lemaitre B (2006). The MAPKKK Mekk1 regulates the expression of Turandot stress genes in response to septic injury in Drosophila. Genes Cells 11, 397–407. [PubMed: 16611243]

Centers for Disease Control and Prevention (2018). Final Annual Maps & Data for 1999–2018. https://www.cdc.gov/westnile/statsmaps/finalmapsdata/index.html.

Choi NH, Lucchetta E, and Ohlstein B (2011). Nonautonomous regulation of Drosophila midgut stem cell proliferation by the insulin-signaling pathway. Proc. Natl. Acad. Sci. U S A 108, 18702–18707. [PubMed: 22049341]

Chotkowski HL, Ciota AT, Jia Y, Puig-Basagoiti F, Kramer LD, Shi P-Y, and Glaser RL (2008). West Nile virus infection of Drosophila melanogaster induces a protective RNAi response. Virology 377, 197–206. [PubMed: 18501400]

Chow CY, Wolfner MF, and Clark AG (2013). Using natural variation in Drosophila to discover previously unknown endoplasmic reticulum stress genes. Proc. Natl. Acad. Sci. U S A 110, 9013–9018. [PubMed: 23667151]

Chow CY, Kelsey KJP, Wolfner MF, and Clark AG (2016). Candidate genetic modifiers of retinitis pigmentosa identified by exploiting natural variation in Drosophila. Hum. Mol. Genet 25, 651–659. [PubMed: 26662796]

Ciota AT, Styer LM, Meola MA, and Kramer LD (2011). The costs of infection and resistance as determinants of West Nile virus susceptibility in Culex mosquitoes. BMC Ecol. 11, 23. [PubMed: 21975028]

Colpitts TM, Cox J, Vanlandingham DL, Feitosa FM, Cheng G, Kurscheid S, Wang P, Krishnan MN, Higgs S, and Fikrig E (2011). Alterations in the Aedes aegypti transcriptome during infection with West Nile, dengue and yellow fever viruses. PLoS Pathog. 7, e1002189. [PubMed: 21909258]

Corby-Harris V, Drexler A, Watkins de Jong L, Antonova Y, Pakpour N, Ziegler R, Ramberg F, Lewis EE, Brown JM, Luckhart S, and Riehle MA (2010). Activation of Akt signaling reduces the prevalence and intensity of malaria parasite infection and lifespan in Anopheles stephensi mosquitoes. PLoS Pathog. 6, e1001003. [PubMed: 20664791]

Darby SM, Miller ML, Allen RO, and LeBeau M (2001). A mass spectrometric method for quantitation of intact insulin in blood samples. J. Anal. Toxicol 25, 8–14. [PubMed: 11216004]

Deddouche S, Matt N, Budd A, Mueller S, Kemp C, Galiana-Arnoux D, Dostert C, Antoniewski C, Hoffmann JA, and Imler J-L (2008). The DExD/H-box helicase Dicer-2 mediates the induction of antiviral activity in Drosophila. Nat. Immunol 9, 1425–1432. [PubMed: 18953338]

Dostert C, Jouanguy E, Irving P, Troxler L, Galiana-Arnoux D, Hetru C, Hoffmann JA, and Imler J-L (2005). The Jak-STAT signaling pathway is required but not sufficient for the antiviral response of Drosophila. Nat. Immunol 6, 946–953. [PubMed: 16086017]

Drexler A, Nuss A, Hauck E, Glennon E, Cheung K, Brown M, and Luckhart S (2013). Human IGF1 extends lifespan and enhances resistance to c falciparum infection in the malaria vector Anopheles stephensi. J. Exp. Biol 216, 208–217. [PubMed: 23255191]

Duffy MR, Chen T-H, Hancock WT, Powers AM, Kool JL, Lanciotti RS, Pretrick M, Marfel M, Holzbauer S, Dubray C, et al. (2009). Zika virus outbreak on Yap Island, Federated States of Micronesia. N. Engl. J. Med 360, 2536–2543. [PubMed: 19516034]

Dyer MD, Murali TM, and Sobral BW (2008). The landscape of human proteins interacting with viruses and other pathogens. PLoS Pathog. 4, e32. [PubMed: 18282095]

Fernandez R, Tabarini D, Azpiazu N, Frasch M, and Schlessinger J (1995). The Drosophila insulin receptor homolog: a gene essential for embryonic development encodes two receptor isoforms with different signaling potential. EMBO J. 14, 3373–3384. [PubMed: 7628438]

Gantz VM, Jasinskiene N, Tatarenkova O, Fazekas A, Macias VM, Bier E, and James AA (2015). Highly efficient Cas9-mediated gene drive for population modification of the malaria vector mosquito Anopheles stephensi. Proc. Natl. Acad. Sci. U S A 112, E6736–E6743. [PubMed: 26598698]

Giannakou ME, Goss M, Jünger MA, Hafen E, Leevers SJ, and Partridge L (2004). Long-lived Drosophila with overexpressed dFOXO in adult fat body. Science 305, 361. [PubMed: 15192154]

Gonzalez I, Mateos-Langerak J, Thomas A, Cheutin T, and Cavalli G (2014). Identification of regulators of the three-dimensional polycomb organization by a microscopy-based genome-wide RNAi screen. Mol. Cell 54, 485–499. [PubMed: 24703951]

Grönke S, Clarke D-F, Broughton S, Andrews TD, and Partridge L (2010). Molecular evolution and functional characterization of Drosophila insulin-like peptides. PLoS Genet. 6, e1000857. [PubMed: 20195512]

Guo J-T, Hayashi J, and Seeger C (2005). West Nile virus inhibits the signal transduction pathway of alpha interferon. J. Virol 79, 1343–1350. [PubMed: 15650160]

Guo C, Zhou Z, Wen Z, Liu Y, Zeng C, Xiao D, Ou M, Han Y, Huang S, Liu D, et al. (2017). Global epidemiology of dengue outbreaks in 1990–2015: a systematic review and meta-analysis. Front. Cell. Infect. Microbiol 7, 317. [PubMed: 28748176]

Hackett BA, and Cherry S (2018). Flavivirus internalization is regulated by a size-dependent endocytic pathway. Proc. Natl. Acad. Sci. U S A 115, 4246–4251. [PubMed: 29610346]

Hadler JL, Patel D, Bradley K, Hughes JM, Blackmore C, Etkind P, Kan L, Getchell J, Blumenstock J, and Engel J; Centers for Disease Control and Prevention (CDC) (2014). National capacity for surveillance, prevention, and control of West Nile virus and other arbovirus infections—United States, 2004 and 2012. MMWR Morb. Mortal. Wkly. Rep 63, 281–284. [PubMed: 24699764]

Haqshenas G, Terradas G, Paradkar PN, Duchemin J-B, McGraw EA, and Doerig C (2019). A role for the insulin receptor in the suppression of dengue virus and Zika virus in Wolbachia-infected mosquito cells. Cell Rep. 26, 529–535.e3. [PubMed: 30650347]

Harrison DA, McCoon PE, Binari R, Gilman M, and Perrimon N (1998). Drosophila unpaired encodes a secreted protein that activates the JAK signaling pathway. Genes Dev. 12, 3252–3263. [PubMed: 9784499]

Harsh S, Ozakman Y, Kitchen SM, Paquin-Proulx D, Nixon DF, and Eleftherianos I (2018). Dicer-2 regulates resistance and maintains homeostasis against Zika virus infection in *Drosophila*. J. Immunol 201, 3058–3072. [PubMed: 30305326]

Hiroyasu A, DeWitt DC, and Goodman AG (2018). Extraction of hemocytes from Drosophila melanogaster larvae for microbial infection and analysis. J. Vis. Exp (135), e57077.

Howick VM, and Lazzaro BP (2017). The genetic architecture of defence as resistance to and tolerance of bacterial infection in Drosophila melanogaster. Mol. Ecol 26, 1533–1546. [PubMed: 28099780]

Hsu SH, Mao WH, and Cross JH (1970). Establishment of a line of cells derived from ovarian tissue of Clex quinquefasciatus Say. J. Med. Entomol 7, 703–707. [PubMed: 5501238]

Hwangbo DS, Gershman B, Tu MP, Palmer M, and Tatar M (2004). Drosophila dFOXO controls lifespan and regulates insulin signalling in brain and fat body. Nature 429, 562–566. [PubMed: 15175753]

Inoue YH, Katsube H, and Hinami Y (2018). Drosophila models to investigate insulin action and mechanisms underlying human diabetes mellitus. Adv. Exp. Med. Biol 1076, 235–256. [PubMed: 29951823]

Kang M-A, Mott TM, Tapley EC, Lewis EE, and Luckhart S (2008). Insulin regulates aging and oxidative stress in Anopheles stephensi. J. Exp. Biol 211, 741–748. [PubMed: 18281336]

Kauffman E, Payne A, Franke MA, Schmid MA, Harris E, and Kramer LD (2017). Rearing of Culex spp. and Aedes spp. mosquitoes. Bio. Protoc 7, e2542.

Kemp C, Mueller S, Goto A, Barbier V, Paro S, Bonnay F, Dostert C, Troxler L, Hetru C, Meignin C, et al. (2013). Broad RNA interference-mediated antiviral immunity and virus-specific inducible responses in Drosophila. J. Immunol 190, 650–658. [PubMed: 23255357]

Kilpatrick AM, Meola MA, Moudy RM, and Kramer LD (2008). Temperature, viral genetics, and the transmission of West Nile virus by Culex pipiens mosquitoes. PLoS Pathog. 4, e1000092. [PubMed: 18584026]

Kingsolver MB, Huang Z, and Hardy RW (2013). Insect antiviral innate immunity: pathways, effectors, and connections. J. Mol. Biol 425, 4921–4936. [PubMed: 24120681]

Kumar M, Roe K, Nerurkar PV, Namekar M, Orillo B, Verma S, and Nerurkar VR (2012). Impaired virus clearance, compromised immune response and increased mortality in type 2 diabetic mice infected with West Nile virus. PLoS ONE 7, e44682. [PubMed: 22953001]

Kumar M, Roe K, Nerurkar PV, Orillo B, Thompson KS, Verma S, and Nerurkar VR (2014). Reduced immune cell infiltration and increased pro-inflammatory mediators in the brain of Type 2 diabetic mouse model infected with West Nile virus. J. Neuroinflammation 11, 80. [PubMed: 24750819]

Lanciotti RS, Ebel GD, Deubel V, Kerst AJ, Murri S, Meyer R, Bowen M, McKinney N, Morrill WE, Crabtree MB, et al. (2002). Complete genome sequences and phylogenetic analysis of West Nile virus strains isolated from the United States, Europe, and the Middle East. Virology 298, 96–105. [PubMed: 12093177]

Laurent-Rolle M, Boer EF, Lubick KJ, Wolfinbarger JB, Carmody AB, Rockx B, Liu W, Ashour J, Shupert WL, Holbrook MR, et al. (2010). The NS5 protein of the virulent West Nile virus NY99 strain is a potent antagonist of type I interferon-mediated JAK-STAT signaling. J. Virol 84, 3503–3515. [PubMed: 20106931]

Lautié-Harivel N, and Thomas-Orillard M (1990). Location of Drosophila C virus target organs in Drosophila host population by an immunofluorescence technique. Biol. Cell 69, 35–39. [PubMed: 2261574]

Lavoy S, Chittoor-Vinod VG, Chow CY, and Martin I (2018). Genetic modifiers of neurodegeneration in a *Drosophila* model of Parkinson's disease. Genetics 209, 1345–1356. [PubMed: 29907646]

Li C-X, Shi M, Tian J-H, Lin X-D, Kang Y-J, Chen L-J, Qin X-C, Xu J, Holmes EC, and Zhang Y-Z (2015). Unprecedented genomic diversity of RNA viruses in arthropods reveals the ancestry of negative-sense RNA viruses. eLife 4, 4.

Lim J, Gowda DC, Krishnegowda G, and Luckhart S (2005). Induction of nitric oxide synthase in Anopheles stephensi by Plasmodium falciparum: mechanism of signaling and the role of parasite glycosylphosphatidylinositols. Infect. Immun 73, 2778–2789. [PubMed: 15845481]

Lin C-C, Chou C-M, Hsu Y-L, Lien J-C, Wang Y-M, Chen S-T, Tsai S-C, Hsiao P-W, and Huang C-J (2004). Characterization of two mosquito STATs, AaSTAT and CtSTAT. Differential regulation of tyrosine phosphorylation and DNA binding activity by lipopolysaccharide treatment and by Japanese encephalitis virus infection. J. Biol. Chem 279, 3308–3317. [PubMed: 14607839]

Loza-Coll MA, Southall TD, Sandall SL, Brand AH, and Jones DL (2014). Regulation of Drosophila intestinal stem cell maintenance and differentiation by the transcription factor Escargot. EMBO J. 33, 2983–2996. [PubMed: 25433031]

Luckhart S, and Riehle MA (2007). The insulin signaling cascade from nematodes to mammals: insights into innate immunity of Anopheles mosquitoes to malaria parasite infection. Dev. Comp. Immunol 31, 647–656. [PubMed: 17161866]

Mackay TFC, Richards S, Stone EA, Barbadilla A, Ayroles JF, Zhu D, Casillas S, Han Y, Magwire MM, Cridland JM, et al. (2012). The Drosophila melanogaster Genetic Reference Panel. Nature 482, 173–178. [PubMed: 22318601]

Marques JT, and Imler J-L (2016). The diversity of insect antiviral immunity: insights from viruses. Curr. Opin. Microbiol 32, 71–76. [PubMed: 27232381]

Martin M, Hiroyasu A, Guzman RM, Roberts SA, and Goodman AG (2018). Analysis of Drosophila STING reveals an evolutionarily conserved antimicrobial function. Cell Rep. 23, 3537–3550.e6. [PubMed: 29924997]

Marzi A, Emanuel J, Callison J, McNally KL, Arndt N, Chadinha S, Martellaro C, Rosenke R, Scott DP, Safronetz D, et al. (2018). Lethal Zika virus disease models in young and older interferon α/β receptor knock out mice. Front. Cell. Infect. Microbiol 8, 117. [PubMed: 29696134]

Mavrouli M, Vrioni G, Kapsimali V, Tsiamis C, Mavroulis S, Pervanidou D, Billinis C, Hadjichristodoulou C, and Tsakris A (2018). Reemergence of West Nile virus infections in southern Greece, 2017. Am. J. Trop. Med. Hyg 100, 420–426.

Molleston JM, and Cherry S (2017). Attacked from all sides: RNA decay in antiviral defense. Viruses 9, 2.

Moon SL, Dodd BJT, Brackney DE, Wilusz CJ, Ebel GD, and Wilusz J (2015). Flavivirus sfRNA suppresses antiviral RNA interference in cultured cells and mosquitoes and directly interacts with the RNAi machinery. Virology 485, 322–329. [PubMed: 26331679]

Moudy RM, Zhang B, Shi P-Y, and Kramer LD (2009). West Nile virus envelope protein glycosylation is required for efficient viral transmission by Culex vectors. Virology 387, 222–228. [PubMed: 19249803]

Mukherjee S, and Hanley KA (2010). RNA interference modulates replication of dengue virus in Drosophila melanogaster cells. BMC Microbiol. 10, 127. [PubMed: 20420715]

Muñoz-Jordán JL, Laurent-Rolle M, Ashour J, Martínez-Sobrido L, Ashok M, Lipkin WI, and García-Sastre A (2005). Inhibition of alpha/beta interferon signaling by the NS4B protein of flaviviruses. J. Virol 79, 8004–8013. [PubMed: 15956546]

Mussabekova A, Daeffler L, and Imler J-L (2017). Innate and intrinsic antiviral immunity in Drosophila. Cell. Mol. Life Sci 74, 2039–2054. [PubMed: 28102430]

Musselman LP, and Kühnlein RP (2018). *Drosophila* as a model to study obesity and metabolic disease. J. Exp. Biol 221 (Pt, Suppl 1), jeb163881. [PubMed: 29514880]

Musselman LP, Fink JL, Grant AR, Gatto JA, Tuthill BF 2nd, and Baranski TJ (2017). A complex relationship between immunity and metabolism in Drosophila diet-induced insulin resistance. Mol. Cell. Biol. 38, e00259–e17. [PubMed: 29084810]

Nag DK, and Kramer LD (2017). Patchy DNA forms of the Zika virus RNA genome are generated following infection in mosquito cell cultures and in mosquitoes. J. Gen. Virol 98, 2731–2737. [PubMed: 29039731]

Nag DK, Brecher M, and Kramer LD (2016). DNA forms of arboviral RNA genomes are generated following infection in mosquito cell cultures. Virology 498, 164–171. [PubMed: 27588377]

Nash D, Mostashari F, Fine A, Miller J, O'Leary D, Murray K, Huang A, Rosenberg A, Greenberg A, Sherman M, et al.; 1999 West Nile Outbreak Response Working Group (2001). The outbreak of West Nile virus infection in the New York City area in 1999. N. Engl. J. Med 344, 1807–1814. [PubMed: 11407341]

Nässel DR, and Vanden Broeck J (2016). Insulin/IGF signaling in Drosophila and other insects: factors that regulate production, release and post-release action of the insulin-like peptides. Cell. Mol. Life Sci 73, 271–290. [PubMed: 26472340]

Nuss AB, Brown MR, Murty US, and Gulia-Nuss M (2018). Insulin receptor knockdown blocks filarial parasite development and alters egg production in the southern house mosquito, Culex quinquefasciatus. PLoS Negl. Trop. Dis 12, e0006413. [PubMed: 29649225]

O'Neill SL, Kittayapong P, Braig HR, Andreadis TG, Gonzalez JP, and Tesh RB (1995). Insect densoviruses may be widespread in mosquito cell lines. J. Gen. Virol 76, 2067–2074. [PubMed: 7636489]

Pabalan N, Chaisri S, Tabunhan S, Tarasuk M, Jarjanazi H, and Steiner T (2017). Associations of tumor necrosis factor-α-308 polymorphism with dengue infection: A systematic review and meta-analysis. Acta Trop. 173, 17–22. [PubMed: 28495402]

Pakpour N, Corby-Harris V, Green GP, Smithers HM, Cheung KW, Riehle MA, and Luckhart S (2012). Ingested human insulin inhibits the mosquito NF-κB-dependent immune response to Plasmodium falciparum. Infect. Immun 80, 2141–2149. [PubMed: 22473605]

Pakpour N, Cheung KW, and Luckhart S (2016). Enhanced transmission of malaria parasites to mosquitoes in a murine model of type 2 diabetes. Malar. J 15, 231. [PubMed: 27102766]

Paradkar PN, Trinidad L, Voysey R, Duchemin J-B, and Walker PJ (2012). Secreted Vago restricts West Nile virus infection in Culex mosquito cells by activating the Jak-STAT pathway. Proc. Natl. Acad. Sci. U S A 109, 18915–18920. [PubMed: 23027947]

Paradkar PN, Duchemin J-B, Voysey R, and Walker PJ (2014). Dicer-2-dependent activation of Culex Vago occurs via the TRAF-Rel2 signaling pathway. PLoS Negl. Trop. Dis. 8, e2823. [PubMed: 24762775]

Petersen LR, Brault AC, and Nasci RS (2013). West Nile virus: review of the literature. JAMA 310, 308–315. [PubMed: 23860989]

Petruzzelli L, Herrera R, Garcia-Arenas R, and Rosen OM (1985a). Acquisition of insulin-dependent protein tyrosine kinase activity during Drosophila embryogenesis. J. Biol. Chem 260, 16072–16075. [PubMed: 3934169]

Petruzzelli L, Herrera R, Garcia R, and Rosen OM (1985b). The insulin receptor of Drosophila melanogaster. Growth Factors Transform. 3, 115–122.

Puig O, Marr MT, Ruhf ML, and Tjian R (2003). Control of cell number by Drosophila FOXO: downstream and feedback regulation of the insulin receptor pathway. Genes Dev. 17, 2006–2020. [PubMed: 12893776]

Rajan A, and Perrimon N (2012). Drosophila cytokine unpaired 2 regulates physiological homeostasis by remotely controlling insulin secretion. Cell 151, 123–137. [PubMed: 23021220]

Reid WR, Zhang L, and Liu N (2015). Temporal gene expression profiles of pre blood-fed adult females immediately following eclosion in the southern house mosquito Culex quinquefasciatus. Int. J. Biol. Sci 11, 1306–1313.

Rios JJ, Perelygin AA, Long MT, Lear TL, Zharkikh AA, Brinton MA, and Adelson DL (2007). Characterization of the equine 2′-5′ oligoadenylate synthetase 1 (OAS1) and ribonuclease L (RNASEL) innate immunity genes. BMC Genomics 8, 313. [PubMed: 17822564]

Rios JJ, Fleming JGW, Bryant UK, Carter CN Jr., Huber JC, Long MT, Spencer TE, and Adelson DL (2010). OAS1 polymorphisms are associated with susceptibility to West Nile encephalitis in horses. PLoS ONE 5, e10537. [PubMed: 20479874]

Rogers SL, and Rogers GC (2008). Culture of Drosophila S2 cells and their use for RNAi-mediated loss-of-function studies and immunofluorescence microscopy. Nat. Protoc 3, 606–611. [PubMed: 18388942]

Rossi ÁD, Faucz FR, Melo A, Pezzuto P, de Azevedo GS, Schamber-Reis BLF, Tavares JS, Mattapallil JJ, Tanuri A, Aguiar RS, et al. (2018). Variations in maternal adenylate cyclase genes are associated with congenital Zika syndrome in a cohort from Northeast, Brazil. J. Intern. Med 285, 215–222. [PubMed: 30222212]

Scherbik SV, and Brinton MA (2010). Virus-induced Ca2+ influx extends survival of west nile virus-infected cells. J. Virol 84, 8721–8731. [PubMed: 20538858]

Schnettler E, Sterken MG, Leung JY, Metz SW, Geertsema C, Goldbach RW, Vlak JM, Kohl A, Khromykh AA, and Pijlman GP (2012). Noncoding flavivirus RNA displays RNA interference suppressor activity in insect and Mammalian cells. J. Virol 86, 13486–13500. [PubMed: 23035235]

Scott JC, Brackney DE, Campbell CL, Bondu-Hawkins V, Hjelle B, Ebel GD, Olson KE, and Blair CD (2010). Comparison of dengue virus type 2-specific small RNAs from RNA interference-competent and -incompetent mosquito cells. PLoS Negl. Trop. Dis 4, e848. [PubMed: 21049014]

Shives KD, Beatman EL, Chamanian M, O'Brien C, Hobson-Peters J, and Beckham JD (2014). West Nile virus-induced activation of mammalian target of rapamycin complex 1 supports viral growth and viral protein expression. J. Virol 88, 9458–9471. [PubMed: 24920798]

Smibert P, Yang J-S, Azzam G, Liu J-L, and Lai EC (2013). Homeostatic control of Argonaute stability by microRNA availability. Nat. Struct. Mol. Biol 20, 789–795. [PubMed: 23708604]

Smith JL, Stein DA, Shum D, Fischer MA, Radu C, Bhinder B, Djaballah H, Nelson JA, Früh K, and Hirsch AJ (2014). Inhibition of dengue virus replication by a class of small-molecule compounds that antagonize dopamine receptor d4 and downstream mitogen-activated protein kinase signaling. J. Virol 88, 5533–5542. [PubMed: 24599995]

Spellberg MJ, and Marr MT, 2nd. (2015). FOXO regulates RNA interference in Drosophila and protects from RNA virus infection. Proc. Natl. Acad. Sci. U S A 112, 14587–14592. [PubMed: 26553999]

Stranger BE, Stahl EA, and Raj T (2011). Progress and promise of genome-wide association studies for human complex trait genetics. Genetics 187, 367–383. [PubMed: 21115973]

Styer LM, Meola MA, and Kramer LD (2007). West Nile virus infection decreases fecundity of Culex tarsalis females. J. Med. Entomol 44, 1074–1085. [PubMed: 18047209]

Subramanian A, Tamayo P, Mootha VK, Mukherjee S, Ebert BL, Gillette MA, Paulovich A, Pomeroy SL, Golub TR, Lander ES, and Mesirov JP (2005). Gene set enrichment analysis: a knowledge-based approach for interpreting genome-wide expression profiles. Proc. Natl. Acad. Sci. U S A 102, 15545–15550. [PubMed: 16199517]

Surachetpong W, Singh N, Cheung KW, and Luckhart S (2009). MAPK ERK signaling regulates the TGF-β1-dependent mosquito response to Plasmodium falciparum. PLoS Pathog. 5, e1000366. [PubMed: 19343212]

Teixeira L, Ferreira A, and Ashburner M (2008). The bacterial symbiont Wolbachia induces resistance to RNA viral infections in Drosophila melanogaster. PLoS Biol. 6, e2.

Terradas G, Joubert DA, and McGraw EA (2017). The RNAi pathway plays a small part in *Wolbachia*-mediated blocking of dengue virus in mosquito cells. Sci. Rep 7, 43847. [PubMed: 28262718]

Tham H-W, Balasubramaniam V, Ooi MK, and Chew M-F (2018). Viral determinants and vector competence of Zika virus transmission. Front. Microbiol 9, 1040. [PubMed: 29875751]

Tsetsarkin KA, Kenney H, Chen R, Liu G, Manukyan H, Whitehead SS, Laassri M, Chumakov K, and Pletnev AG (2016). A Full-length infectious cDNA clone of Zika virus from the 2015 epidemic in Brazil as a genetic platform for studies of virus-host interactions and vaccine development. MBio 7, e01114–e01116. [PubMed: 27555311]

U.S. Department of Health and Human Services (2009). Biosafety in Microbiological and Biomedical Laboratories (U.S. Department of Health and Human Services).

van Rij RP, Saleh M-C, Berry B, Foo C, Houk A, Antoniewski C, and Andino R (2006). The RNA silencing endonuclease Argonaute 2 mediates specific antiviral immunity in Drosophila melanogaster. Genes Dev. 20, 2985–2995. [PubMed: 17079687]

Wang JB, Lu H-L, and St Leger RJ (2017). The genetic basis for variation in resistance to infection in the Drosophila melanogaster genetic reference panel. PLoS Pathog. 13, e1006260. [PubMed: 28257468]

Webster CL, Waldron FM, Robertson S, Crowson D, Ferrari G, Quintana JF, Brouqui J-M, Bayne EH, Longdon B, Buck AH, et al. (2015). The discovery, distribution, and evolution of viruses associated with Drosophila melanogaster. PLoS Biol. 13, e1002210. [PubMed: 26172158]

West C, and Silverman N (2018). p38b and JAK-STAT signaling protect against Invertebrate iridescent virus 6 infection in Drosophila. PLoS Pathog. 14, e1007020. [PubMed: 29746571]

Xavier-Carvalho C, Cardoso CC, de Souza Kehdy F, Pacheco AG, and Moraes MO (2017). Host genetics and dengue fever. Infect. Genet. Evol 56, 99–110. [PubMed: 29133029]

Xia Z, Xu G, Yang X, Peng N, Zuo Q, Zhu S, Hao H, Liu S, and Zhu Y (2017). Inducible TAP1 negatively regulates the antiviral innate immune response by targeting the TAK1 complex. J. Immunol 198, 3690–3704. [PubMed: 28356387]

Xu J, Hopkins K, Sabin L, Yasunaga A, Subramanian H, Lamborn I, Gordesky-Gold B, and Cherry S (2013). ERK signaling couples nutrient status to antiviral defense in the insect gut. Proc. Natl. Acad. Sci. U S A 110, 15025–15030. [PubMed: 23980175]

Yamaguchi T, Fernandez R, and Roth RA (1995). Comparison of the signaling abilities of the Drosophila and human insulin receptors in mammalian cells. Biochemistry 34, 4962–4968. [PubMed: 7711018]

Yan R, Small S, Desplan C, Dearolf CR, and Darnell JE Jr. (1996). Identification of a Stat gene that functions in Drosophila development. Cell 84, 421–430. [PubMed: 8608596]

Yasunaga A, Hanna SL, Li J, Cho H, Rose PP, Spiridigliozzi A, Gold B, Diamond MS, and Cherry S (2014). Genome-wide RNAi screen identifies broadly-acting host factors that inhibit arbovirus infection. PLoS Pathog. 10, e1003914. [PubMed: 24550726]

Zhang B, Salituro G, Szalkowski D, Li Z, Zhang Y, Royo I, Vilella D, Díez MT, Pelaez F, Ruby C, et al. (1999). Discovery of a small molecule insulin mimetic with antidiabetic activity in mice. Science 284, 974–977. [PubMed: 10320380]

Zhang W, Thompson BJ, Hietakangas V, and Cohen SM (2011). MAPK/ERK signaling regulates insulin sensitivity to control glucose metabolism in Drosophila. PLoS Genet. 7, e1002429. [PubMed: 22242005]

Zhang H, Zhang C, Tang H, Gao S, Sun F, Yang Y, Zhou W, Hu Y, Ke C, Wu Y, et al. (2018). CD2-associated protein contributes to hepatitis C virus propagation and steatosis by disrupting insulin signaling. Hepatology 68, 1710–1725. [PubMed: 29729186]

Zhou F, and Agaisse H (2012). Jak-Stat Signaling: From Basics to Disease (Springer).

Zhou S, Morozova TV, Hussain YN, Luoma SE, McCoy L, Yamamoto A, Mackay TFC, and Anholt RRH (2016). The genetic basis for variation in sensitivity to lead toxicity in Drosophila melanogaster. Environ. Health Perspect 124, 1062–1070. [PubMed: 26859824]

Highlights

- Identified insulin-like receptor as anti-flaviviral in a screen of adult *Drosophila*

- Insulin signaling inhibits antiviral RNAi while activating the JAK/STAT pathway

- Flavivirus replication is reduced in mosquito cells primed with mammalian insulin

- West Nile virus titer is reduced in *Culex* mosquitoes that are fed mammalian insulin
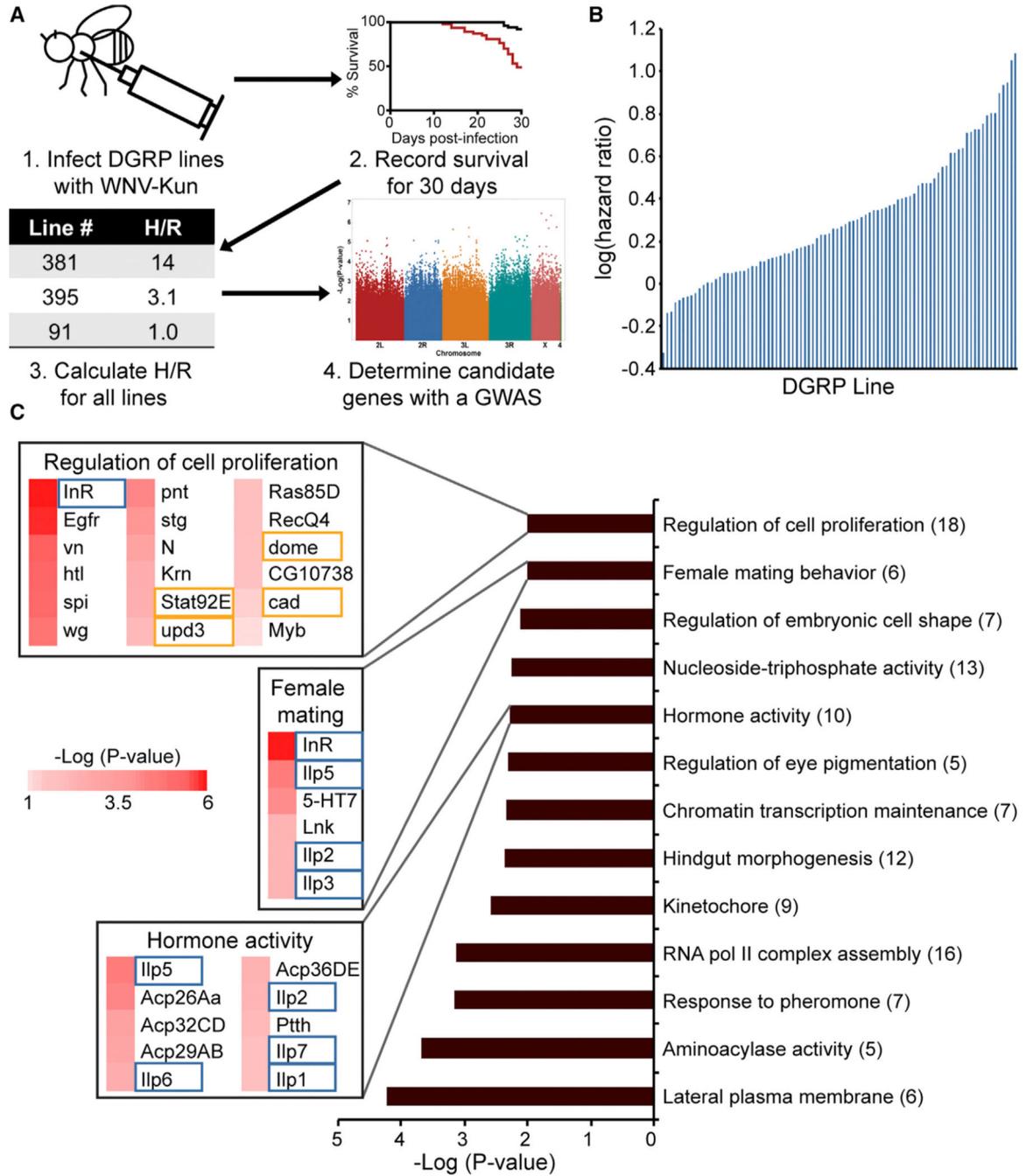
Figure 1. A Genetic Screen of *D. melanogaster* Identified Candidate Genes Involved in the *D. melanogaster* Response to WNV-Kun

(A) Schematic of the screen and downstream analysis.

(B) Survival of each DGRP line, measured by log(hazard ratio).

(C) Gene set enrichment analysis (GSEA) using genes for all variants and their associated p values from the GWAS. Heatmap data represent GWAS variant p values, while the bar graph indicates the GSEA p value and the number of genes enriched for each GO category in parentheses. Genes indicated in orange boxes are components of the JAK/STAT pathway, and genes indicated by blue boxes are components of the insulin signaling pathway.
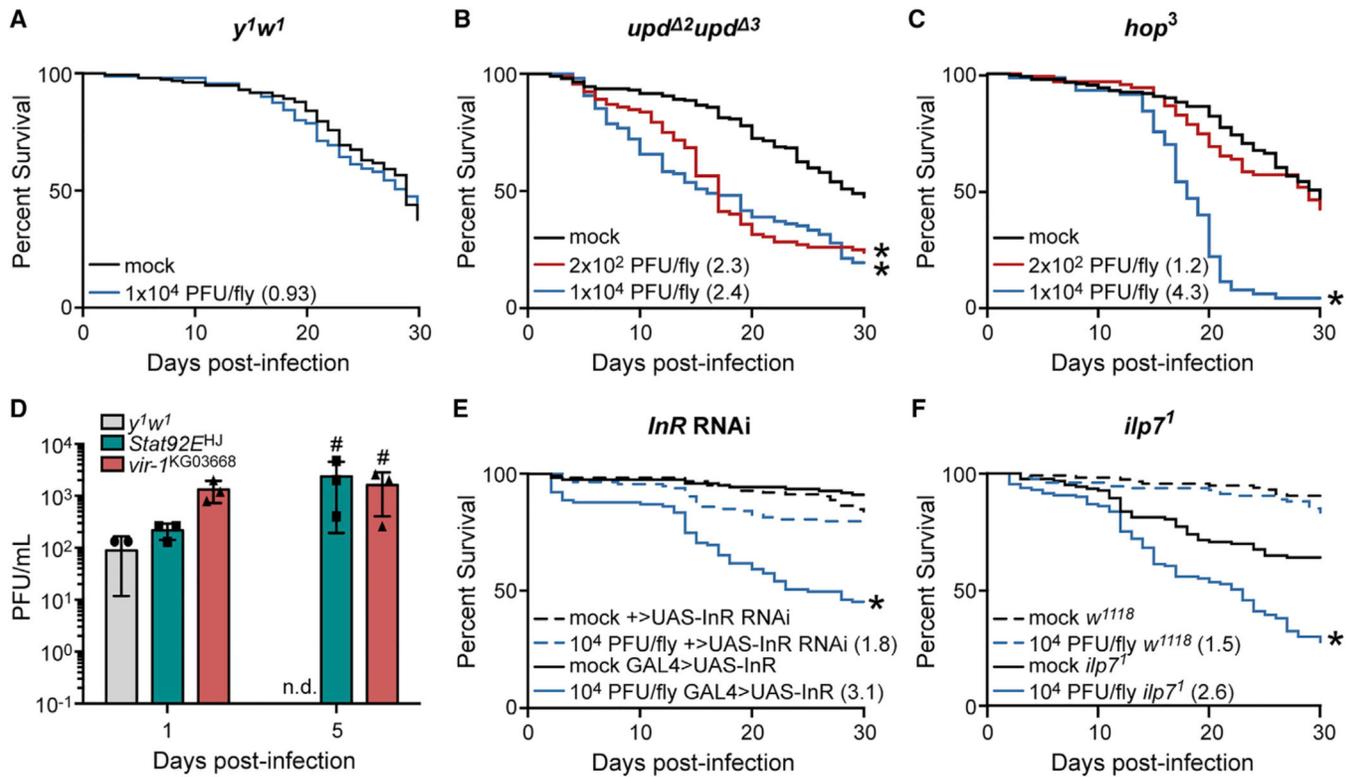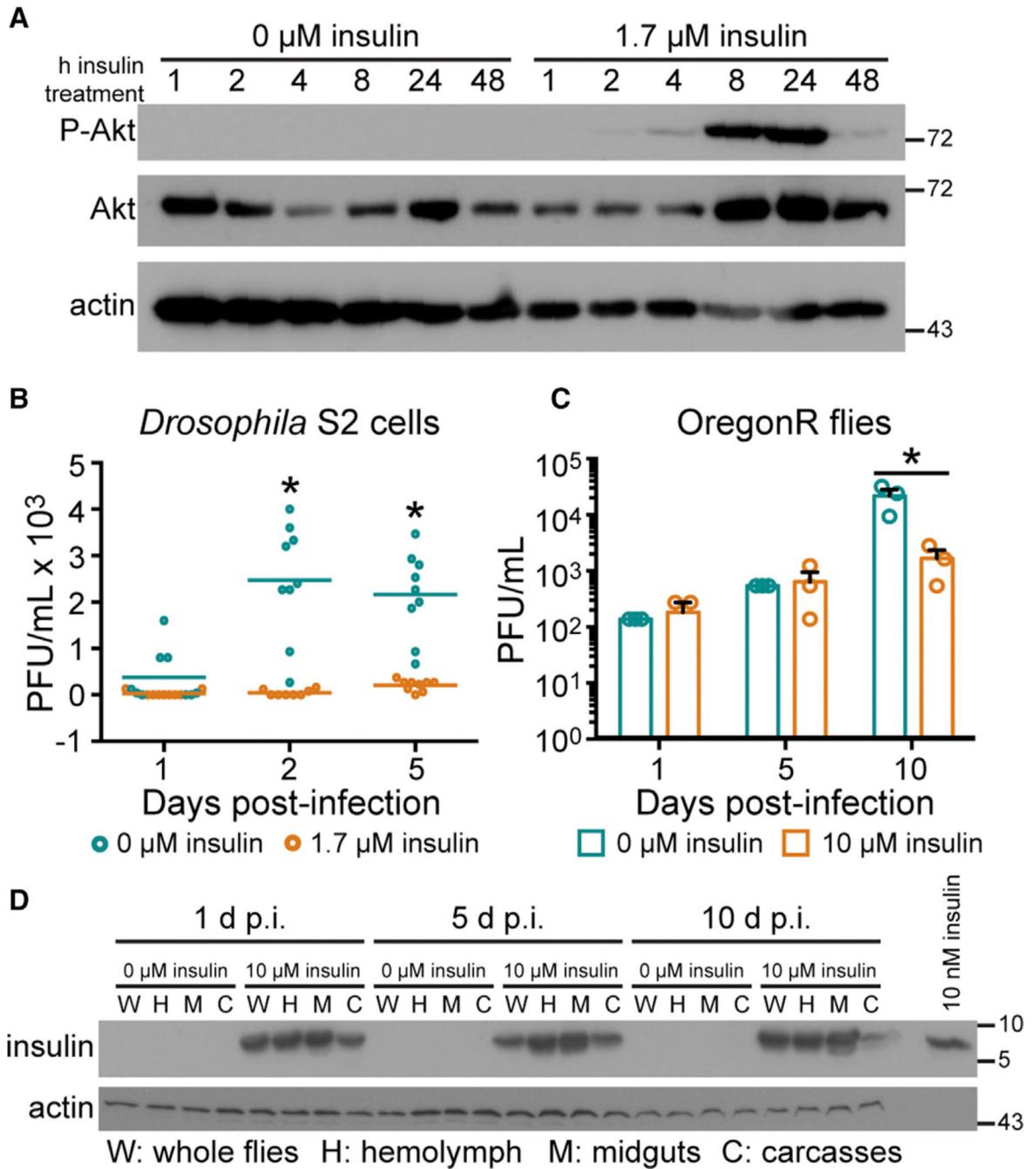
Figure 2. Components of the JAK/STAT and Insulin Signaling Pathways Are Necessary for *D. melanogaster* Survival against WNV-Kun Infection

(A–C) Mutants in the genes (B) *upd2* and *upd3* and (C) *hop* are susceptible to WNV-Kun infection compared with the (A) y^1w^1 isotype control.

(D) WNV-Kun titer is higher in *Stat92E* and *vir-1* mutant flies relative to the y^1w^1 isotype control at 5 days post-infection (#p < 0.05, Mann-Whitney test).

(E) *InR* knockdown and (F) *ilp7[1]* mutant flies are susceptible to WNV-Kun compared with the sibling or background controls. Hazard ratio for each infection group is indicated in parenthesis, and statistical significance from the control group is indicated with an asterisk (*p < 0.05, log-rank test).

Each survival curve represents two (B and C) or three (A, E, and F) independent experiments of >40 flies that were combined for a final survival curve. For titer results (D), marker shapes represent biological replicates, the bar represents the mean, and error bars represent SDs. Samples for which virus was not detected are indicated by "n.d." Titer data are representative of duplicate independent experiments.

A

0 µM insulin | 1.7 µM insulin

h insulin treatment: 1 2 4 8 24 48 | 1 2 4 8 24 48

P-Akt — 72

Akt — 72

actin — 43

B *Drosophila* S2 cells

C OregonR flies

○ 0 µM insulin   ○ 1.7 µM insulin

□ 0 µM insulin   □ 10 µM insulin

D

1 d p.i. | 5 d p.i. | 10 d p.i.

0 µM insulin | 10 µM insulin | 0 µM insulin | 10 µM insulin | 0 µM insulin | 10 µM insulin | 10 nM insulin

W H M C W H M C W H M C W H M C W H M C W H M C

insulin — 10, 5

actin — 43

W: whole flies   H: hemolymph   M: midguts   C: carcasses

Figure 3. The *D. melanogaster* Insulin Signaling Pathway Is Activated by Vertebrate Insulin, Which Is Antiviral to WNV-Kun

(A) Akt is phosphorylated and activated in *D. melanogaster* S2 cells when treated with bovine insulin.

(B) WNV-Kun titer is reduced in S2 cells primed with 1.7 µM bovine insulin for 24 h prior to infection (MOI = 0.01 PFU/cell).

(C) WNV-Kun titer is reduced in *D. melanogaster* on a diet of 10 µM bovine insulin (*p < 0.05, unpaired t test). Open circles represent biological replicates. Horizontal lines or bars represent the mean. Error bars represent SDs.

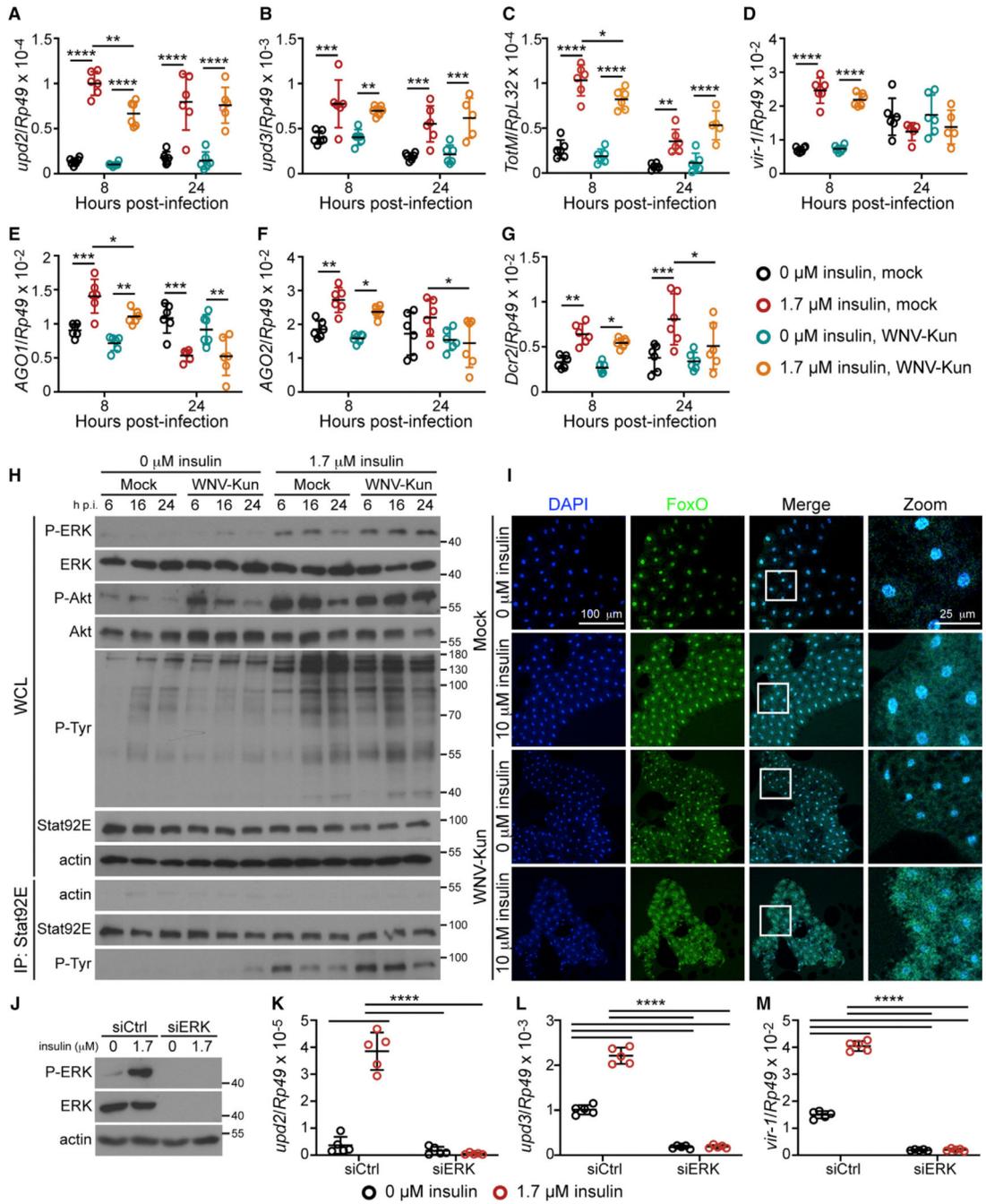(D) Ingested insulin disseminates from the midgut into the hemolymph in flies on a diet of 10 μM bovine insulin.

Results are representative of duplicate (A and D) or triplicate (B and C) independent experiments.

Figure 4. Insulin Priming Activates Antiviral Pathways in *D. melanogaster*

(A–G) Induction of genes within the JAK/STAT pathway, (A) *upd2*, (B) *upd3*, (C) *TotM*, and (D) *vir-1*, and the RNAi pathway, (E) *AGO1*, (F) *AGO2*, and (G) *Dcr2*, were measured using qRT-PCR following priming of *D. melanogaster* S2 cells with 1.7 μM insulin and mock or WNV-Kun infection.

(H) Levels of ERK, Akt, and Stat92E phosphorylation were measured using western blot following insulin treatment and mock or WNV-Kun infection of S2 cells.

(I) FoxO localization in the larval fat body was determined by confocal microscopy using third-instar larvae on a standard cornmeal diet with or without 10 μM bovine insulin and mock- or WNV-Kun-infected for 4 h.

(J–M) ERK was knocked down in S2 cells (J), and transcript levels of (K) *upd2*, (L) *upd3*, and (M) *vir-1* were measured using qRT-PCR (*p < 0.05, **p < 0.01, ***p < 0.001, and ****p < 0.0001, ANOVA with correction for multiple comparisons).

Open circles represent biological replicates. Horizontal black bars represent the mean. Error bars represent SDs. Results are representative of duplicate independent experiments.
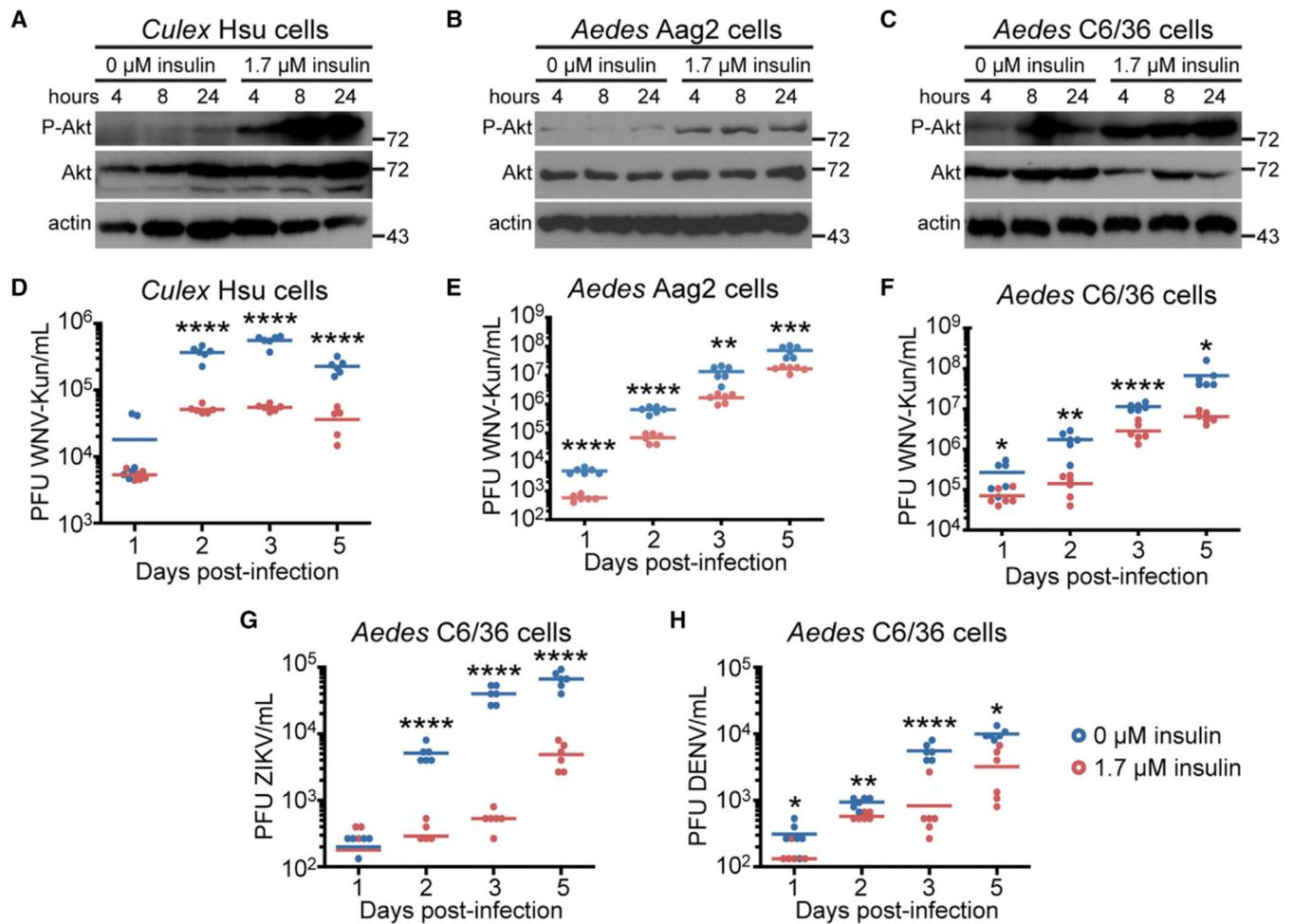
Figure 5. Insulin Priming Reduces Flavivirus Titer in *Cx. quinquefasciatus*, *Ae. aegypti*, and *Ae. albopictus* Cells

(A–C) Akt is phosphorylated and activated by insulin priming in (A) *Cx. quinquefasciatus* Hsu cells, (B) *Ae. aegypti* Aag2 cells, and (C) *Ae. albopictus* C6/36 cells.

(D–H) Insulin priming reduces WNV-Kun titer in (D) Hsu, (E) Aag2, and (F) C6/36 cells and (G) Zika virus and (H) dengue virus titer in C6/36 cells (MOI = 0.01 PFU/cell) (*p < 0.05, **p < 0.01, ***p < 0.001, ****p < 0.0001, unpaired t test).

Open circles represent biological replicates. Horizontal bars represent the mean. Error bars represent SDs. Results are representative of triplicate independent experiments.
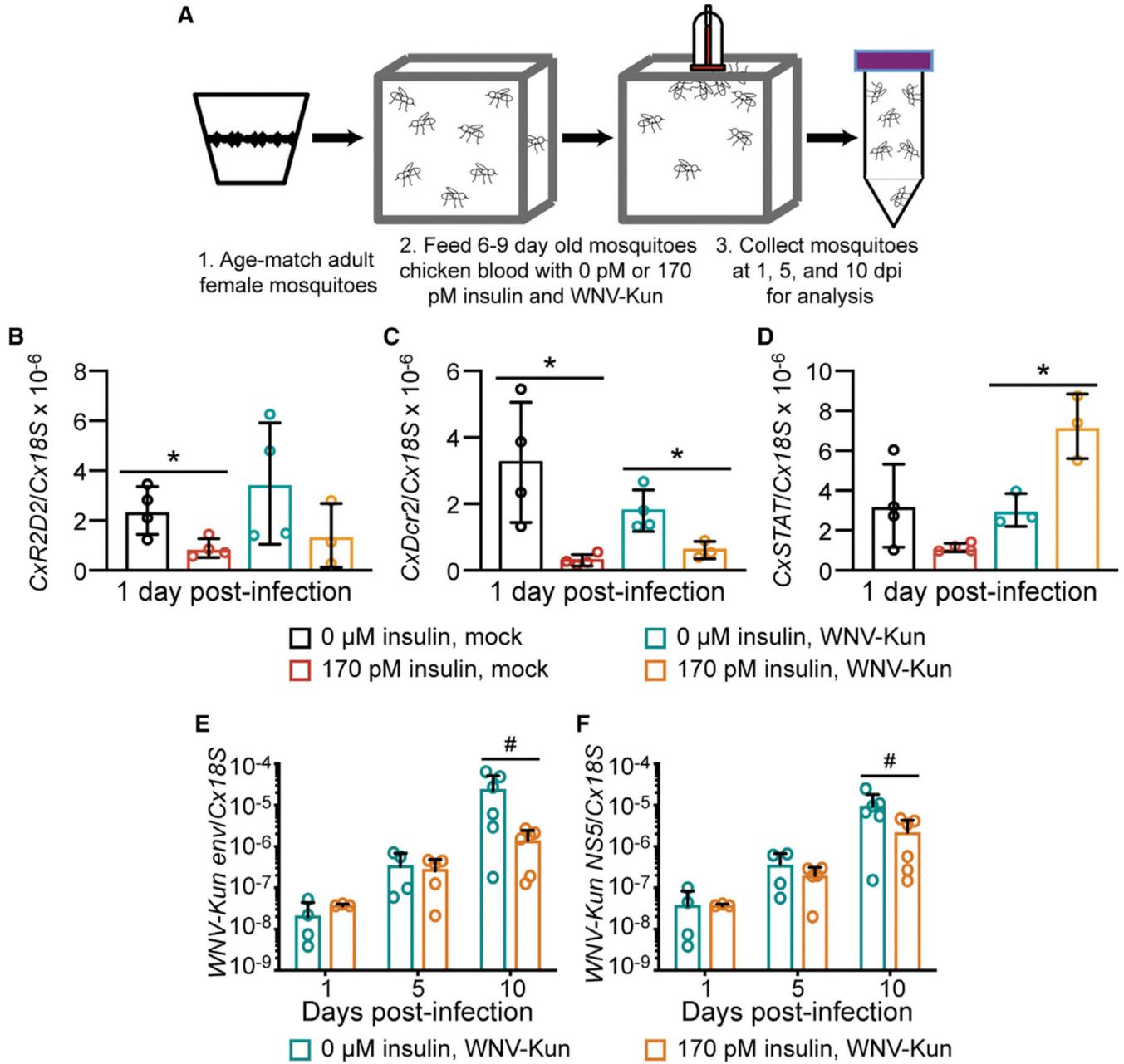
Figure 6. Insulin Activates the Antiviral Response in Adult Female *Cx. quinquefasciatus*

(A) Schematic illustrating process of age-matching pupae into adults, feeding female mosquitoes a blood meal of chicken blood with or without insulin or WNV-Kun, and collecting adults for analysis post-infection.

(B–F) Induction of (B) *CxR2D2*, (C) *CxDcr2*, (D) *CxSTAT*, (E) WNV-Kun *envelope* (*env*), and (F) *NS5* genes were measured using qRT-PCR following blood feeding of *Cx. quinquefasciatus* (*p < 0.05, unpaired t test; or #p < 0.05, Mann-Whitney test). Circles represent biological replicates. Bars represent the mean. Error bars represent SDs. Results are representative of duplicate independent experiments.
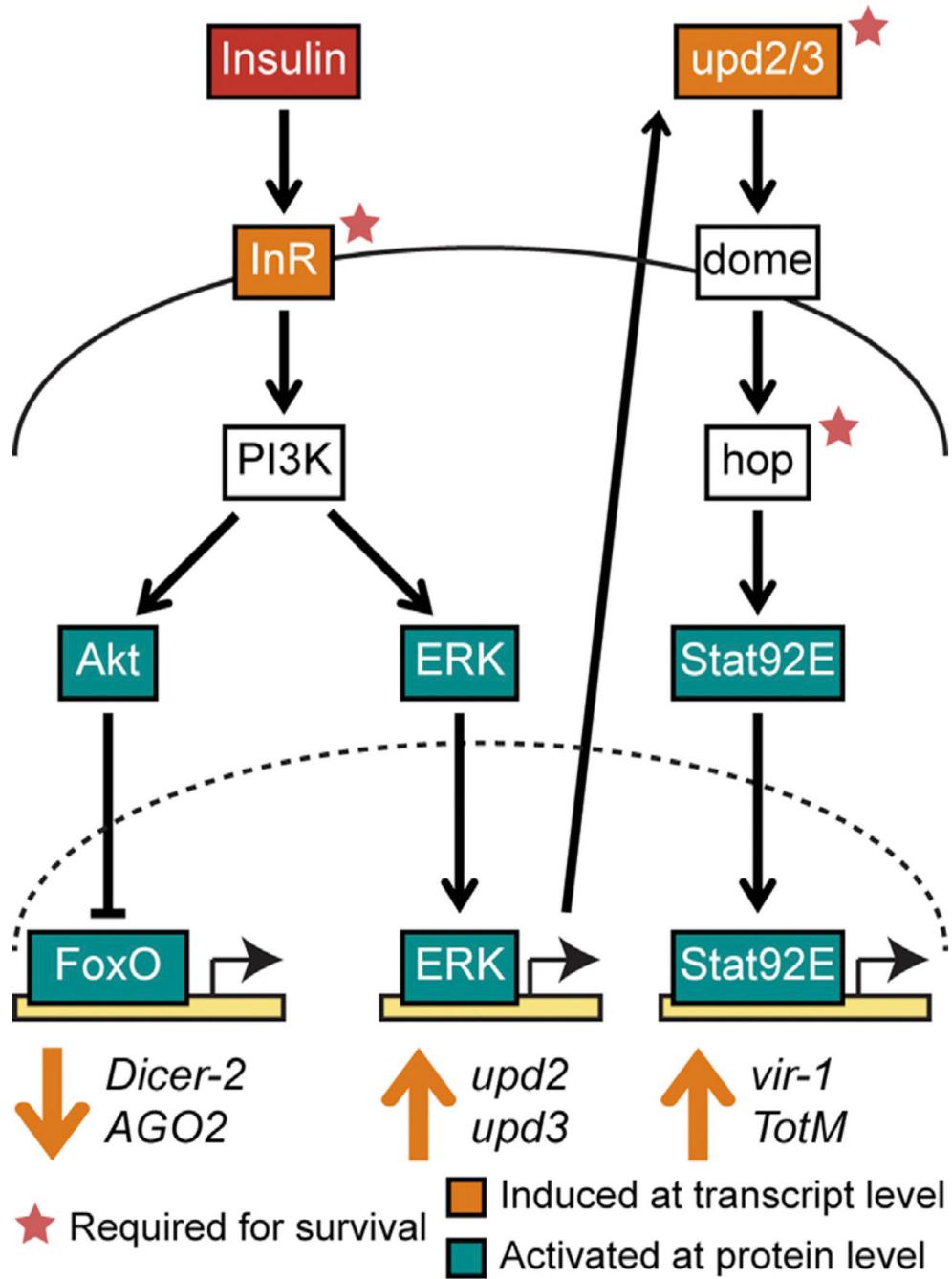
Figure 7. Schematic of Immune Signaling during Insulin Priming in Insects

Insulin (red box) binds to the insulin-like receptor (InR), activating a signaling cascade that inhibits FoxO-dependent transcription of RNAi components and reduces RNAi-dependent antiviral immunity. Proposed networked regulation of insulin and JAK/STAT signaling includes activation of ERK downstream of PI3K and increased expression of *upd2/3*, suggesting a control point for insulin-enhanced JAK/STAT signaling. Signaling components denoted by pink stars were important for *D. melanogaster* survival during WNV-Kun

infection. Components indicated by orange boxes were induced at the transcript level by insulin treatment, and those indicated by teal boxes were activated at the protein level.

KEY RESOURCES TABLE

REAGENT or RESOURCE	SOURCE	IDENTIFIER
Antibodies		
Rabbit monoclonal anti-phospho-Akt (Ser473)	Cell Signaling	Cat#4060
		RRID:AB_2315049
Rabbit monoclonal anti-Akt (pan) (C67E7)	Cell Signaling	Cat#4691
		RRID:AB_915783
Goat polyclonal anti-Stat (dN-17)	Santa Cruz	Cat#15708
		RRID:AB_661405
Rabbit monoclonal anti-p44/42 MAPK (Erk1/2) (137F5)	Cell Signaling	Cat#4695
		RRID:AB_390779
Rabbit monoclonal anti-phospho-p44/42 MAPK (Erk1/2) (Thr202/Tyr204) (D13.14.4E)	Cell Signaling	Cat#4370
		RRID:AB_2315112
Rabbit monoclonal anti-phospho-Tyr (P-Tyr-1000) MultiMab	Cell Signaling	Cat#8954
		RRID:AB_2687925
Rabbit polyclonal anti-actin	Sigma	Cat#A2066
		RRID:AB_476693
Mouse monoclonal anti-insulin	Novus Biologicals	Cat#NBP2–34260
		RRID:AB_2811080
Anti-rabbit IgG (H+L) HRP conjugate	Promega	Cat#4011
		RRID:AB_430833
Anti-goat IgG (H+L) HRP conjugate	Jackson Immunoresearch	Cat#705–035–147
		RRID:AB_2313587
Bacterial and Virus Strains		
West Nile virus-Kunjin	Laboratory of Robert Tesh	MRM16 strain
Zika virus	Laboratory of Sonja Best	Paraiba strain
Dengue virus 2	Laboratory of Sonja Best	New Guinea C strain (BEI NR-84)
Biological Samples		
Chicken Blood	Colorado Serum Company	Cat#31141
Hog sausage casing	C&L Locker Co. (Local butcher)	N/A
Culex quinquefasciatus eggs (Strain JHB)	BEI Resources	NR-43025
Chemicals, Peptides, and Recombinant Proteins		
ERK chemical inhibitor U0126	Cell Signaling	Cat#9903
Insulin from bovine pancreas	Sigma	Cat#10516
T7 RiboMAX Express Large Scale RNA Production System	Promega	Cat#P1320
Cellfectin II	ThermoFisher	Cat#10362100
Experimental Models: Cell Lines		
Cercopithecus aethiops: Cell line Vero	ATCC	CCL-81

REAGENT or RESOURCE	SOURCE	IDENTIFIER
Aedes albopictus: Cell line C6/36	ATCC	CRL-1660
Culex quinquefasciatus: Cell line Hsu	Hsu et al., 1970	
D. melanogaster: Cell line S2: S2-DGRC	Laboratory of Lucy Cherbas	FlyBase: FBtc0000006
Aedes aegypti: Cell line Aag2wMel.tet	Terradas et al., 2017	Laboratory of Scott O'Neill
Experimental Models: Organisms/Strains		
D. melanogaster: Isogenic control line: $y^1 w^1$	Bloomington Drosophila Stock Center	BDSC: 1495; Flybase: FBst0001495
D. melanogaster: wild-type line: Oregon-R-C	Bloomington Drosophila Stock Center	BDSC: 5; Flybase: FBst0000005
D. melanogaster: wild-type line: w^{1118}	Bloomington Drosophila Stock Center	BDSC: 5905; Flybase: FBst0005905
D. melanogaster: GFP-tagged FoxO: w^{1118}; PBac{$y^{+mDint2}w^{+mC}$ = foxo-GFP.FLAG}VK00037	Bloomington Drosophila Stock Center	BDSC#38644; Flybase: FBst0038644
D. melanogaster: *Stat92e* mutant: $y^1 w^*$; $ry^* e^1$ Stat92E^{HJ}/TM3, Sb^1	Bloomington Drosophila Stock Center	BDSC#24510; Flybase: FBst0024510
D. melanogaster: *hop* mutant: y^{1}w*hop^3/FM7c	Bloomington Drosophila Stock Center	BDSC#8495; Flybase: FBst0008495
D. melanogaster: *vir-1* mutant: $y^1 w^{67c23}$; p{$y^{+mDint2}w^{BR.E.BR}$ = SUPor-P}vir-1^{KG03668}	Bloomington Drosophila Stock Center	BDSC#13292; Flybase: FBst0013292
D. melanogaster: *Dicer-2* mutant: y^{d2} w^{1118} P{ey-FLP.N}2; Dcr-2^{L811fsX}; P{Dcr-2$^{E1371K.t7.2}$}3	Bloomington Drosophila Stock Center	BDSC#32064; Flybase: FBst0032064
D. melanogaster: *AGO2* mutant: w^{1118}; AGO2^{454}/TM3, Sb^1 Ser^1	Bloomington Drosophila Stock Center	BDSC#36512; Flybase: FBst0036512
D. melanogaster: *upd2* and *upd3* mutant: w* upd2 upd3	Bloomington Drosophila Stock Center	BDSC#55729; Flybase: FBst0055729
D. melanogaster: *InR* RNAi: y^1v^1; P{TRiP.JF01482}attP2	Bloomington Drosophila Stock Center	BDSC#31037; Flybase: FBst0031037
D. melanogaster: *ilp7* mutant: w^{1118} TI{$w^{+mW.hs}$ = TI}Ilp7^1	Bloomington Drosophila Stock Center	BDSC#30887; Flybase: FBst 0030887
D. melanogaster: Actin driver line: y^{1}w*;P{Act5C-GAL4} 25FO1/CyO,y$^+$	Bloomington Drosophila Stock Center	BDSC: 4414 Flybase: FBst0004414
D. melanogaster: *Tak1* mutant: Tak1^{2527}	Bloomington Drosophila Stock Center	BDSC#58809; Flybase: FBst0058809
D. melanogaster: *EGFR* mutant: Egfr^{t1} bw^1/CyO	Bloomington Drosophila Stock Center	BDSC#2079; Flybase: FBst0002079
Oligonucleotides		
DmRp49 qRT-PCR:	Integrated DNA Technologies	Spellberg and Marr, 2015
Forward: CCACCAGTCGGATCGATATGC		
Reverse: CTCTTGAGAACGCAGGCGACC		
DmDcr2 qRT-PCR:	Integrated DNA Technologies	Spellberg and Marr, 2015
Forward: GTATGGCGATAGTGTGACTGCGAC		
Reverse: GCAGCTTGTTCCGCAGCAATATAGC		
DmAGO1 qRT-PCR:	Integrated DNA Technologies	Spellberg and Marr, 2015
Forward: GCTACAAGCCCCACCGCATC		
Reverse: CCCGATTTGCCGCTCTGCTC		
DmAGO2 qRT-PCR:	Integrated DNA Technologies	Spellberg and Marr, 2015

REAGENT or RESOURCE	SOURCE	IDENTIFIER
Forward: CCGGAAGTGACTGTGACAGATCG		
Reverse: CCTCCACGCACTGCATTGCTCG		
DmInR qRT-PCR:	Integrated DNA Technologies	This study
Forward: TTCACCCGCTACGCTATCTT		
Reverse: GCTGCAGAGCGACTTCTTAAA		
DmVir-1 qRT-PCR:	Integrated DNA Technologies	Deddouche et al., 2008
Forward: GATCCCAATTTTCCCATCAA		
Reverse: GATTACAGCTGGGTGCACAA		
DmUpd2 qRT-PCR:	Integrated DNA Technologies	This study
Forward: CCTATCCGAACAGCAATGGT		
Reverse: CTGGCGTGTGAAAGTTGAGA		
DmUpd3 qRT-PCR:	Integrated DNA Technologies	This study
Forward: GCCCTCTTCACCAAACTGAA		
Reverse: TCGCCTTGCACAGACTCTTA		
Cx18S qRT-PCR:	Integrated DNA Technologies	Reid et al., 2015
Forward: CGCGGTAATTCCAGCTCCACTA		
Reverse: GCATCAAGCGCCACCATATAGG		
CxR2D2 qRT-PCR:	Integrated DNA Technologies	Paradkar et al., 2012
Forward: GCAGGAAATTTGCGCCCGCC		
Reverse: CAAGTCTGGCCAAGCGCCGT		
CxDcr2 qRT-PCR:	Integrated DNA Technologies	This study
Forward: TGCAAGGGCTGGAGATAAAG		
Reverse: TCAGGGTTTTCGTTTTACGG		
CxSTAT qRT-PCR:	Integrated DNA Technologies	Lin et al., 2004 and this study
Forward: CAGATTCTGCACATCCAGCCGTTCACG		
Reverse: GGCTTGTTCGGGTACAGGT		
WNV-Kun *env* qRT-PCR:	Integrated DNA Technologies	This study
Forward: TGGAGCATTCCGCTCATTGT		
Reverse: GAGGAACGTGAGGGCTATGG		
WNV-Kun *NS5* qRT-PCR:	Integrated DNA Technologies	This study
Forward: CTCTGCAAGCTCACTGGTCA		
Reverse: TGTCCAAAAGGGGTGGTGTC		
DmERK (*rolled*) dsRNA:	Integrated DNA Technologies	Gonzalez et al., 2014
Forward: T7 + CTTTGGATTGGCTCGTATTG		
Reverse: T7 + AGGATCATAATATTGCTCTAAATAG		
T7 = TAATACGACTCACTATAGG		
Software and Algorithms		
Genome-Wide Association Study	Chow et al., 2016	N/A
Gene Set Enrichment Analysis (GSEA)	Subramanian et al., 2005	N/A

REAGENT or RESOURCE	SOURCE	IDENTIFIER
D. melanogaster gene ontology categories	FlyBase	Version fb_2016_04
Prism	GraphPad	Version 8